SPECIAL
GDIS Drought Worldwide
COLLECTION

Drought over East Asia: A Review

LIXIA ZHANG

LASG, Institute of Atmospheric Physics, Chinese Academy of Sciences, Beijing, and Collaborative Innovation Center on Forecast and Evaluation of Meteorological Disasters, Nanjing University of Information Science and Technology, Nanjing, China

TIANJUN ZHOU

LASG, Institute of Atmospheric Physics, Chinese Academy of Sciences, and Joint Center for Global Change Studies, Beijing, China

(Manuscript received 8 April 2014, in final form 3 January 2015)

ABSTRACT

East Asia is greatly impacted by drought. North and southwest China are the regions with the highest drought frequency and maximum duration. At the interannual time scale, drought in the eastern part of East Asia is mainly dominated by two teleconnection patterns (i.e., the Pacific–Japan and Silk Road teleconnections). The former is forced by SST anomalies in the western North Pacific and the tropical Indian Ocean during El Niño decaying year summers. The precipitation anomaly features a meridional tripolar or sandwich pattern. The latter is forced by Indian monsoon heating and is a propagation of stationary Rossby waves along the Asian jet in the upper troposphere. It can significantly influence the precipitation over north China. Regarding the long-term trend, there exists an increasing drought trend over central parts of northern China and a decreasing tendency over northwestern China from the 1950s to the present. The increased drought in north China results from a weakened tendency of summer monsoons, which is mainly driven by the phase transition of the Pacific decadal oscillation. East Asian summer precipitation is poorly simulated and predicted by current state-of-the-art climate models. Encouragingly, the predictability of atmospheric circulation is high because of the forcing of ENSO and the associated teleconnection patterns. Under the SRES A1B scenario and doubled CO_2 simulations, most climate models project an increasing drought frequency and intensity over southeastern Asia. Nevertheless, uncertainties exist in the projections as a result of the selection of climate models and the choice of drought index.

1. Introduction

Drought, characterized by below-normal precipitation over a period of months to years, has become an increasing concern in recent years. Of all natural disasters, the economic and environmental consequences of drought are among the most serious, because of its longevity and widespread spatial extent. Associated with global warming, the occurrence and durations of drought show an increasing tendency. Its impact is becoming more and more severe, particularly to the people of East Asia (Zhai et al. 2010).

East Asia, which mainly includes China, Japan, Korea Peninsula, and Mongolia, is highly impacted by drought every year. East Asia is dominated by different climate zones. Its western part, located in the north of the Qinghai–Xizang Plateau, is a typical arid and semiarid area. In contrast, east of 102.5°E is the typical monsoon domain. The drought and flooding over this region are closely related to the variability of the East Asian monsoon system, which features strong southerly wind in summer and northerly wind in winter. The location of each region can be found in Fig. 1a. Since China occupies over 80% of the area and 90% of the population of East Asia, we focus mainly on drought occurrence in China in this paper, while the review is also partly expanded to other regions of East Asia.

The historical record shows that drought frequency over north China (the blue region in Fig. 1a) is much higher than that of flooding, because of the local deficiency of rainfall and high temperatures (Zhang et al. 2003). Since the 1960s, and especially since the 1980s,

Corresponding author address: Dr. Tianjun Zhou, LASG, Institute of Atmospheric Physics, Chinese Academy of Sciences, P.O. Box 9804, Beijing 100029, China.
E-mail: zhoutj@lasg.iap.ac.cn

DOI: 10.1175/JCLI-D-14-00259.1

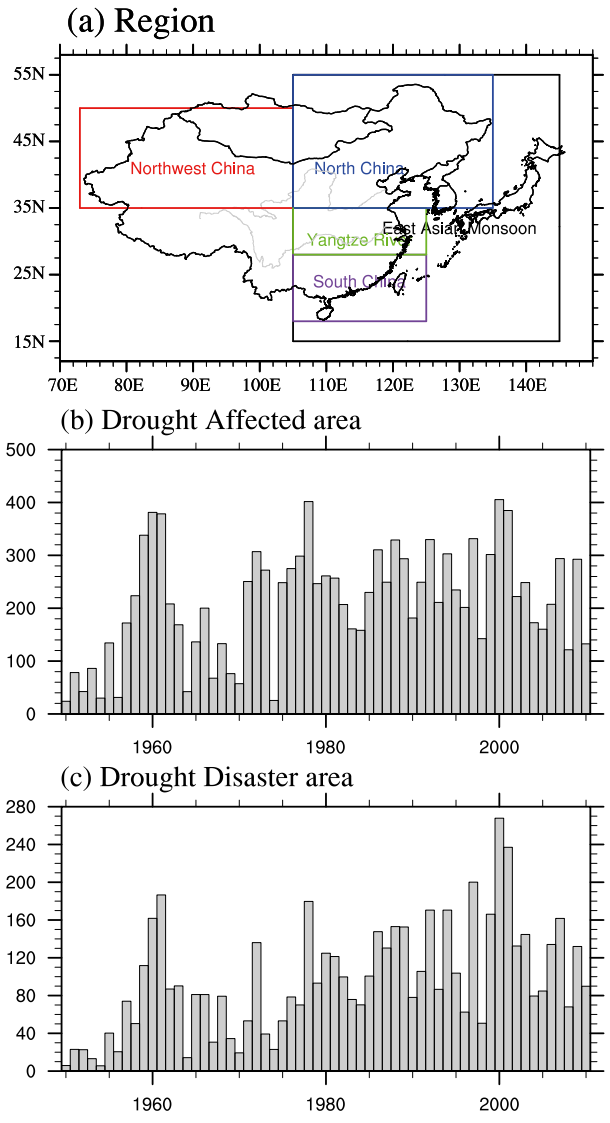

FIG. 1. (a) The location of each region used in this paper. (b),(c) The yearly drought-affected area and drought disaster area (1×10^4 ha) during 1950–2010, respectively. The datasets of agricultural areas influenced by drought are from the China planting industry information network.

north China has experienced consecutive drought periods, two of which caused a drying up of the Yellow River in 1972 and 1997 (Zhang et al. 2009). Besides north China, southwestern China has also experienced a severe drought lasting from autumn 2009 to spring 2010, during which time approximately 21 million people were short of drinking water and economic losses reached nearly USD 30 billion (Yang et al. 2012). According to statistics, droughts in China cause grain losses of 20–25 $\times$ 10^9 kg, which effects 200–300 million people, and economic losses of CNY 15–20 billion every year (Zhang et al. 2008).

Since the 1970s, aridity over north China has increased substantially, and the extreme drought frequency is increasing in the central part of northern China, northeast China, and the eastern part of northwest (NW) China (Ma and Fu 2006). Because of the increasing drought, the grassland area of Jilin Province (41°–46°N, 122°–131°E) is decreasing at a rate of 2.8% per year, the semiarid boundary of northern China has shifted southeastward during the last 50 years (1950–98), and the discharge of the Yellow River is decreasing (Ma and Fu 2006). Owing to the destruction of forest cover and a history of poor water management, severe drought in the Yunnan Province (20°–30°N, 98°–105°E) of southwest China has been exacerbated for many years (Qiu 2010).

To monitor and study drought and its variation, many drought indices have been defined. An extensive listing of available indices can be found in Heim (2000). Evaluations of drought indices have been performed by Keyantash and Dracup (2002) and Dai (2011a). Reviews on four categories (meteorology, agriculture, hydrology, and socioeconomics) of drought indices used in China have been carried out by many scientists (Yuan and Zhou 2004; J. Wang et al. 2007; Yao et al. 2007). The most commonly used drought indices over East Asia include the precipitation anomaly percentage (PA), the Palmer drought severity index (PDSI), standardized precipitation index (SPI), composite drought index (CDI), and effective drought index (EDI); their strengths and weaknesses for describing local drought are listed in Table 1.

The main advantage of PA is that it can reflect droughts induced by precipitation anomalies. However, it does not consider evaporation and is highly dependent on the climatology rainfall. The unified classification is not appropriate in NW China, where precipitation is extremely heterogeneous (Zhang et al. 1998). PDSI is a meteorological drought index used widely throughout the world and provides a good reflection of soil moisture deficit or surplus (Palmer 1965; Dai et al. 1998, 2004). To date, PDSI has mostly been used in drought assessment, comparisons, and assessments of spatial and temporal changes of drought. Because of the complicated topography of East Asia, the determination and computation of empirical parameters in PDSI is difficult. It is hard to use PDSI for drought monitoring and application in East Asia. In China, SPI can detect droughts and wet periods at different time scales, while it is greatly affected by the length of the precipitation record and probability distributions. Specifically, precipitation is seasonal in nature, and zero values are common in NW China, where the calculated SPI values at short time scales may not be normally distributed because of the highly skewed underlying precipitation distribution and the limitation of the fitted gamma distribution (Mishra and Singh 2010). CDI, a combination of SPI and

relative moisture, is provided by the National Climate Center (NCC) of the China Meteorological Administration to monitor provincial meteorological drought (Zou and Zhang 2008). Comparisons between drought events at different regions are allowed. EDI, which is calculated by using daily precipitation and can measure drought onset and end dates, is a widely used drought index over the Korea Peninsula and Japan.

Since different climatic zones dominate East Asia, the topography and vegetation types differ greatly among these climatic zones, the distribution of precipitation is inhomogeneous. It is difficult to use one drought index to reasonably represent all features of droughts over the whole of East Asia. In northwest China, which is an arid/semiarid area, no drought index is able to represent the drought types and severity levels (J. Wang et al. 2007).

Great efforts have been devoted to monitoring, understanding, and forecasting drought over East Asia. The scientific committee of the Global Drought Information System (GDIS) sponsored a special collection of review papers that address the causes of drought worldwide. This paper is a part of that collection. In this paper, we review the occurrence of severe drought over East Asia, the key regional circulation in East Asia related to drought and possible mechanisms, the long-term trend of drought severity and extent, and predictions and projections of drought over East Asia.

The remainder of the paper is organized as follows. The data and drought indices used in this paper are introduced in section 2. Sections 3 and 4 introduce the occurrence of severe droughts in East Asia and the climate states of East Asian drought, respectively. In section 5 the physical mechanisms responsible for drought occurrence at the interannual time scale are summarized. Section 6 reviews the long-term trend of droughts over East Asia and possible mechanisms. Section 7 discusses predictability and projections. And finally, a summary is provided in section 8.

2. Data and drought indices

Two observational precipitation datasets are used here: the Global Precipitation Climatology Project (GPCP) from 1979 to 2012 with a resolution of 2.5° × 2.5° (Adler et al. 2003) and the latest version of the Climatic Research Unit (CRU) dataset from 1950 to 2009 with a resolution of 0.5° × 0.5° (Mitchell and Jones 2005).

The reanalysis dataset used here is the National Centers for Environmental Prediction (NCEP)–National Center for Atmospheric Research (NCAR) reanalysis for 1950–2009 (Kalnay et al. 1996).

Two drought indices are used in this study: a self-calibrating PDSI (sc-PDSI; Dai 2011b) and SPI. Because PDSI is dependent on climatologically appropriate rainfall, which is different in each region of China, it shows some deficiencies in depicting East Asian drought, as described in Table 1. The sc-PDSI calibrates the PDSI by using local coefficients; thus, the sc-PDSI is more comparable spatially than the original PDSI. In addition, the Penman–Monteith method is considered to be the most physics based and reliable method for calculating potential evapotranspiration (Dai 2011b). Therefore, an sc-PDSI with the Penman–Monteith equation is used in this paper. The sc-PDSI data used in the study are from the Climate Data Guide website (https://climatedataguide.ucar.edu/climate-data/palmer-drought-severity-index-pdsi), with a 2.5° × 2.5° resolution. Since SPI is one of the operational monitoring indices used in the NCC, we use SPI to show the climatic characteristics of drought over China. The SPI is calculated by using monthly CRU precipitation dataset, with a resolution 0.5° × 0.5°. In the review of interannual variability of East Asian drought, SPI for 1 month time scale (SPI-1) is employed. In studying the long-term changes of East Asian drought, 12-month SPI (SPI-12) is used here and is interpolated into 2.5° × 2.5° grid to compare with sc-PDSI, because sc-PDSI is unable to depict droughts on time scales shorter than 12 months when monthly PDSI values are used (Vicente-Serrano et al. 2010).

To show the impact of historical droughts that have occurred in China, a dataset of agricultural areas influenced by drought from the China planting industry information network is used here (http://202.127.42.157/moazzys/zaiqing.aspx). The drought- (disaster-) affected areas are those areas in which a crop yield reduction due to drought occurred in more than 10% (30%) of normal years.

3. Historical review of severe drought over East Asia

Using the area percentage of eastern China under very dry conditions based on the historical records and instrumental data of the past 500 years, Shen et al. (2007) identified three exceptional drought events that occurred over the monsoon region of China: 1586–89, 1638–41, and 1965–66. During these droughts, more than 40% of the area was affected, and there was a 50% or more reduction of precipitation in the drought center. Each of the events developed first in north China and then expanded to the Yangtze River valley along 30°N and then on into south China. The drought of 1638–41 occurred under the background of the Little Ice Age, when the East Asian summer monsoon circulation was generally weak (Man et al. 2012).

Drought years and the associated impacts in China for the period 1900–2012 are summarized in Table 2

TABLE 1. Most commonly used meteorological drought indices to monitor and study drought over East Asia.

Index name	Calculation	Drought classification	Strength	Weakness	Applied area
Precipitation anomaly percentage	Precipitation anomaly percentage against 30-yr climatological mean.	There are three drought classifications for monthly, seasonal, and annual mean precipitation anomalies. For the seasonal drought, Near normal: 25 to −25 Mild: −50 to −25 Moderate: −70 to −50 Severe: −80 to −70 Extreme: −80 or less	It can reflect the drought induced by precipitation anomaly.	There is no consideration of evaporation and it is highly dependent on the climatological rainfall. The unified classification is not appropriate in NW China, where precipitation is extremely heterogeneous (Zhang et al. 1998).	It is used in the semihumid and semiarid regions when the air temperature is higher than 10°C (Zhang et al. 2006).
Palmer drought severity index (Palmer 1965; Dai et al. 1998, 2004)	Departure of moisture balance from a normal condition based on a 2-layer bucket-type water balance model.	Near normal: −0.49 to 0.49 Incipient dry spell: −0.5 to −0.99 Mild: −1.0 to −1.99 Moderate: −2.0 to −2.99 Severe: −3.0 to −3.99 Extreme:−4.0 or less	It considers both water supply and demand and provides a good reflection of soil moisture deficit or surplus.	Determination of empirical parameters is difficult. Because the empirical constants in the index are based on the climate conditions in the United States, it is not suited for East Asia. The absolute value of PDSI exaggerates the real drought intensity in the Huaihe River valley (Wang and Xu 2012). According to the observational data in China, the PDSI is modified by many studies (An and Xing 1986; Liu et al. 2004; Yang et al. 2005a,b).	Frequently used in drought study over China, such as the drought variations for1951–2003 (Zou et al. 2005), its relation to streamflow (Zhai et al. 2010), and some regional drought assessments.
Standardized precipitation index (McKee et al. 1993; Edwards and McKee 1997)	Fitting and transforming a long-term precipitation record into a normal distribution with respect to the SPI, which has zero mean and unit std dev.	Near normal: −0.50 to 0.50 Abnormal: −0.79 to −0.51 Moderate: −1.29 to −0.80 Severe: −1.59 to −1.30 Extreme: −1.99 to −1.60 Exceptional: −2.00 or less	It can be calculated for a variety of time scales to monitor short-term water supplies and long-term water resources.	In NW China, zero values of precipitation are common. The calculated SPI values at short time scales may not be normally distributed.	Studying wet and dry conditions over the Pearl River basin in south China and Xinjiang Province in northwestern China (Zhang et al. 2009, 2012) and the assessment of drought hazard (He et al. 2011).
Composite drought index (Zou and Zhang 2008)	Combination of 30-day mean and 90-day mean standardized precipitation index and 30-day mean relative moisture.	Near normal: −0.6 to 0.6 Abnormal: −1.2 to −0.6 Moderate:−1.8 to −1.2 Severe:−2.4 to −1.8 Extreme: −2.4 or less	It can standardize drought on different time scales and allows comparisons between drought events at different stations.	When monitoring the 2009/10 drought over China, an ‘‘unreasonable drought aggravate’’ problem emerged.	It is provided by the NCC and used in provincial meteorological monitoring (Liu et al. 2009; Li et al. 2009; Yang and Xie 2009; Zou and Zhang 2008).

TABLE 1. (*Continued*)

Index name	Calculation	Drought classification	Strength	Weakness	Applied area
Effective drought index (Byun and Wilhite 1999)	It is defined as a lack of precipitation in comparison with the climatological average.	Near normal: −1.0 to 1.0 Moderate: −1.5 to −1.0 Severe drought: −2.0 to −1.5 Extreme: −2.0 or less	Can determine drought onset and end dates and is more precise than SPI in quantifying drought (Morid et al. 2006; Pandey et al. 2007; Kim et al. 2009).		It is widely used in the study of drought occurring in the Korea Peninsula and Japan (Kim and Byun 2009; Kim et al. 2011; Lee et al. 2012; Oh et al. 2014).

(Zhang et al. 2009). The droughts that occurred in the 1920s and the 1940s caused huge damage to the society and have been described in many Chinese pieces of literature and journals (e.g., Wang et al. 2000, 2002; Gong 2007; Zhang et al. 2009). Although rain gauge observations were rare in China prior to 1950, these two severe droughts were evident in the limited observational data (see Fig. 1 of Zhou et al. 2009a). Based on soil moisture, a total of 76 droughts were identified during 1950–2006 for drought areas greater than 150 000 km^2 and durations longer than 3 months. They identified the five most prominent droughts (i.e., 1997–2003, 1964–70, 1974–79, 2004–06, and 1962–64); and the drought of 1997–2003 was the most severe and lasted for 76 months (Wang et al. 2011). The yearly drought-affected areas and drought disaster–affected areas in China for the period 1949–2012 are shown in Fig. 1. The time series of drought-affected areas shows severe drought in 1959, 1960, 1961, 1972, 1978, 1986, 1988, 1992, 1994, 1997, 1999, 2000, 2001, and 2010, with a drought area larger than 300×10^4 ha. The top three years in terms of the maximum drought disaster area are 2000, 2001, and 1997, in which the area was greater than 200×10^4 ha. Judging by its impact, the 1965–66 drought identified by Shen et al. (2007) is not among the most severe drought events. Nevertheless, if we compare the drought area percentage ranked by the severity of certain drought indices, the drought of 1965–66 can be identified: for example, the 3-month standardized precipitation index (SPI3), the 3-month reconnaissance drought index (RDI3), and the 3-month standardized precipitation evapotranspiration index (SPEI3) in Xu et al. (2014).

From 1902 to 2009 the most extreme droughts in Japan occurred in 1939–41 and 1984–85 (Lee et al. 2012). An examination of the spatial and temporal changes of EDI over the Korea Peninsula showed that extreme droughts in the Korea Peninsula occurred in 1927–30, 1938–45, 1951–52, 1967–69, and 1994–96, mainly caused by consecutive shortages of summer rainfall lasting for two or more years (Kim et al. 2011). In 1939–45 and 1994–96, both Japan and the Korea Peninsula underwent severe drought periods (Lee et al. 2012; Kim et al. 2011).

4. Climate states of East Asian drought

Most of East Asia is dominated by monsoonal circulation, and precipitation shows large seasonal variation. The summer monsoon rainfall accounts for 40%–50% (60%–70%) of the annual precipitation in south (north) China [Gong (2007); see Zhou et al. (2009a) for a review]. The percentage contribution to annual total rainfall accounted by each season and the associated climatological distribution of seasonal mean wind at 850 hPa are shown

TABLE 2. Drought years over East Asia from 1900 to 2010. The events from 1900 to 2006 were obtained from the appendix table of Zhang et al. (2009).

Year(s)	Region	Impacts
1900	Exceptional drought over China	Huanghe River and Wei River basin dried up. No rainfall from spring to autumn.
1928–29	Exceptional drought over China	About 120 million people, 30% of the total population, subjected to drought. Two million people died of starvation.
1936	Extreme drought over China	Drought over north China and the Yangtze–Huaihe River valley lasted for 3 years from 1934 to 1936. Rivers were dried up, inducing failed harvest.
1942	Severe drought over most regions of China	No rainfall from spring to autumn. Rivers dried up and crops withered. Numerous people died of starvation and plague.
1959	Drought over central China in summer and autumn	Deficient rainfall occurred over the Wei River basin, the middle and lower reaches of the Yangtze River, and the north part of Nanling mountain. The drought-induced disaster area was 1.7×10^4 km^2 in Hubei Province.
1960	Drought over north China	Drought lasted to early summer. The Huanghe River and eight rivers in Shandong Province dried up. About 20×10^4 km^2 affected.
1961	Drought over north China in spring	A 16×10^4 km^2 drought area. Yield of wheat in Henan Province halved and reached lowest ever level.
1972	Exceptional drought over China	Yield of northeast China only 20% of a normal year. Water level dropped and the lower reaches of the Huanghe River dried up for 20 days.
1978	Exceptional drought over most regions of China	Greatly reduced agricultural production because drought mostly occurred in grain-producing areas.
1992	Drought over north China in winter and spring and south China in autumn	Event lasted from autumn 1991 to July 1992. Less rainfall seen in north China, inducing losses of at least CNY 9 billion.
1994	Drought over the Yangtze–Huaihe River valley in autumn	Drought in the Anhui and Jiangsu Provinces most severe, resulting in losses of CNY 20 billion.
1997	Drought over north China in summer	The Huanghe River dried up for 222 days, which was the longest time since 1949. The Huaihei River also dried up for 122 days.
1999	Severe drought over north China	Most parts of north China suffered winter–spring and summer–autumn consecutive droughts.
2000	Drought over north China in spring and summer	About 40.54×10^4 km^2 impacted, inducing losses of CNY 10 billion.
2001	Drought over north China and Yangtze River valley from spring to summer	Drought-induced disaster area was 38.47×10^4 km^2, and 32.95 million people in 17 provinces were short of water.
2003	Drought over the south of the Yangtze River and south China in autumn	Resulted in 100×10^6 kg crop yield losses and CNY 5.8 billion economic losses.
2006	Drought over the Sichuan Province and Chongqing in autumn	High temperatures and drought caused CNY 21.6 billion economic losses. Agricultural disaster area was 3.39×10^4 km^2, and 18 million people suffered shortages of water.
2009–10	North China, Hebei, Shanxi, Liaoning, southwest China, Yunnan, Guizhou, Guangxi, and Sichuan (Qiu 2010).	Reservoirs were severely affected with a 20% reduction in nationwide hydroelectrical production, and large cropland sectors of northern and eastern China experienced up to 8 months of persistently stressed vegetation (Barriopedro et al. 2012).

in Fig. 2. In winter (Fig. 2a), East Asia is dominated by northerly wind along its east coastline. Thus, cold and dry air prevails in winter and the precipitation is very small. Most regions over China undergo very dry conditions. The largest precipitation percentage is 15%–20% and is seen over south China. In the spring (Fig. 2b), the rainfall in south China accounts for 35%–40%, which is close to that of summer. However, the precipitation percentage in southwestern and northeastern China is still very small. Considering the dry conditions in winter, spring drought in these two regions tends to occur. In summer (Fig. 2c), southwesterly wind flow is seen through eastern China, the Korea Peninsula, and Japan. East of 102.5°E is the typical monsoon domain. The summer monsoon rainband is dominated by the anticyclone circulation over the western Pacific (the western Pacific subtropical high). The seasonal stepwise northward migration of the subtropical high dominates the northward migration of the monsoon rainband over East Asia (see Fig. 2 of Zhou et al. 2009a). Except for south China, in most regions the

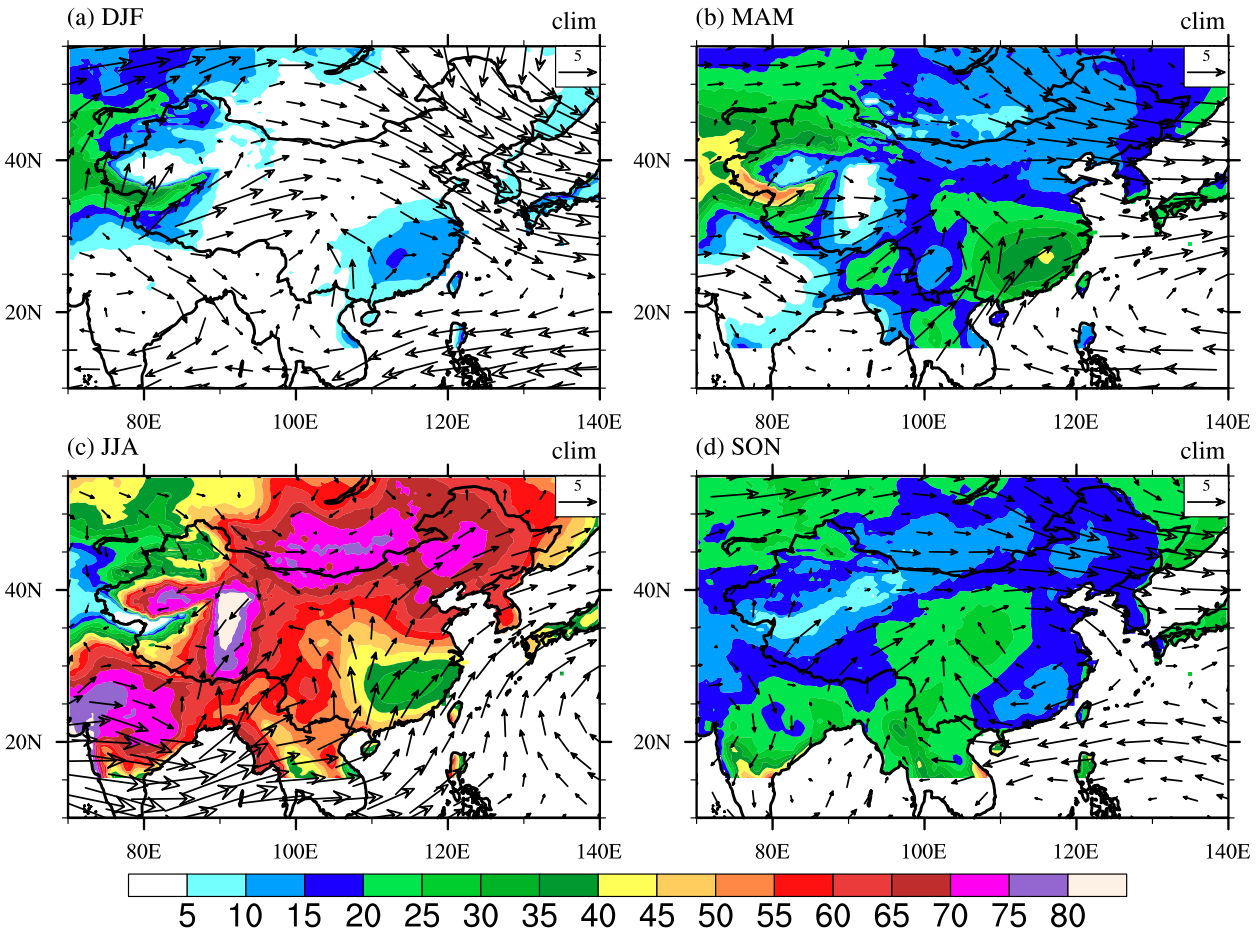

FIG. 2. Percentage of total rainfall (shaded, %) accounted for by each season and the associated climatological distribution of seasonal mean wind at 850 hPa (vectors, $m\,s^{-1}$) for (a) December–February (DJF), (b) March–May (MAM), (c) June–August (JJA), and (d) September–November (SON) for 1950–2009 derived from CRU and NCEP–NCAR.

summer rainfall explains the largest percentage of annual rainfall. In autumn (Fig. 2d), northeast wind starts to prevail along the East Asia coast, and rainfall starts to reduce with the largest precipitation percentage over central China (20°–40°N, 90°–110°E). The monsoon precipitation is impacted by the western Pacific subtropical high through modulating water vapor transport (Zhou and Yu 2005). Following the seasonal withdrawal of the western Pacific subtropical high, drought shows obviously seasonal variation. This climate background provides a useful reference for our following discussion on the drought.

The frequencies of drought (defined as sc-PDSI < -2 and SPI-12 < -0.8, respectively) that occurred over China in the period 1950–2009 are shown in Fig. 3. According to the sc-PDSI data, there is high drought frequency over northern and southwestern China (Fig. 3a). The central value is located in north China, with a frequency greater than 50% (Fig. 3a). The maximum drought durations (Fig. 3c) show similar patterns to drought frequency. The maximum duration time is longer than 54 months over the whole 60 years. Southwest China witnesses a comparable maximum duration as north China, but with less frequency. This is consistent with Zhang et al. (2009), who used the daily composite-drought index developed by the NCC. The largest center for drought frequency and maximum drought duration derived from SPI-12 is also seen over north China, but with less magnitude than that in sc-PDSI (Figs. 3c,d). However, there is another maximum drought duration center derived from SPI-12 located in northwest China. This difference is related to the definition of SPI, which only uses precipitation.

Based on EDI, Oh et al. (2014) analyzed drought characteristics over East Asia. They showed that short-term (<200 days) droughts mainly occur in spring and summer, whereas long-term droughts (≥200 days) mainly start in autumn and winter. The highest frequency of short-term droughts is seen in south China. In the lower reaches of the Yangtze River, central China, the Korea

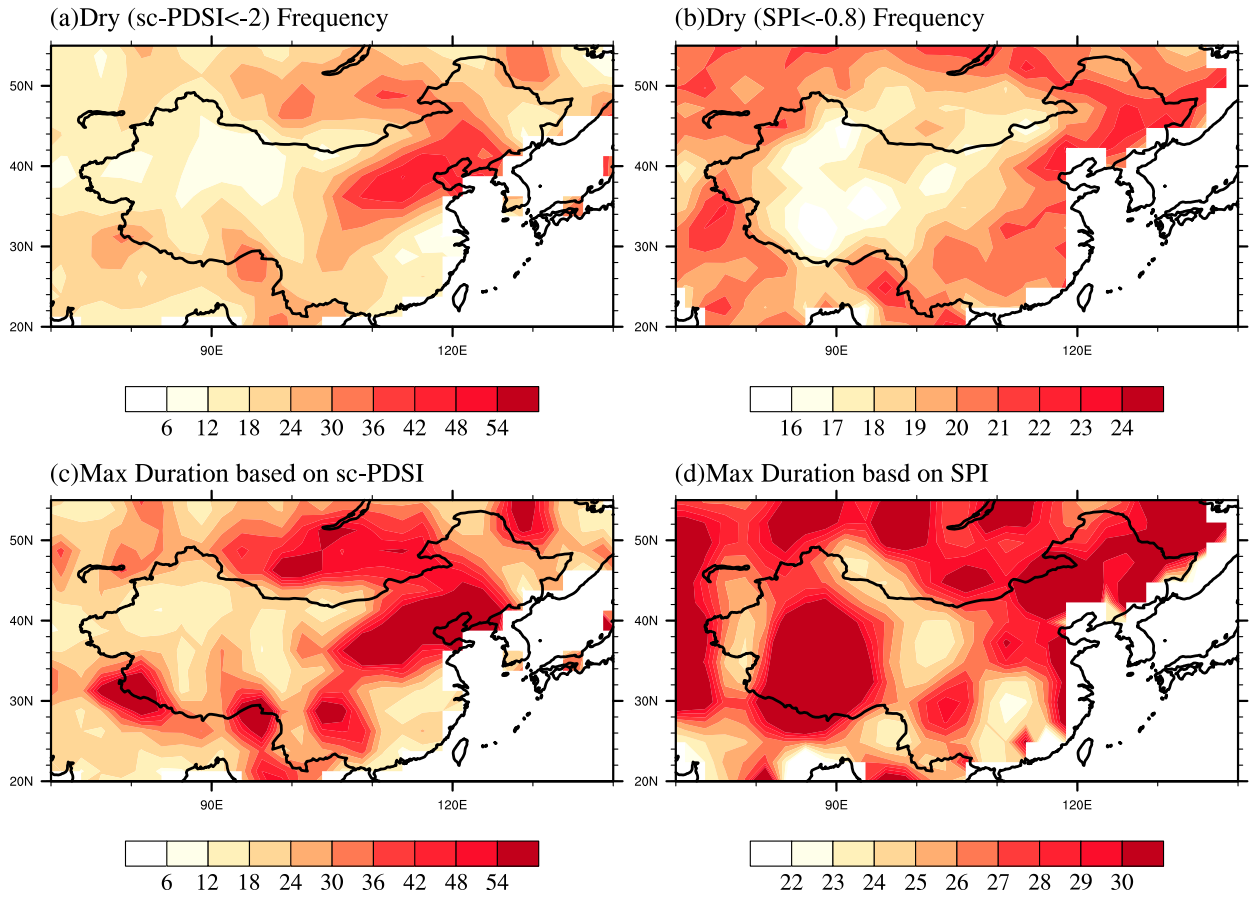

FIG. 3. The (a),(b) drought frequency (%) and (c),(d) maximum drought duration (months) derived from (left) sc-PDSI and (right) SPI-12 during 1950–2009.

Peninsula, and central–south Japan, short-term droughts occur more frequently than longer-term droughts, but in NW China, the middle reaches of the Yangtze River, northeast China, and north Japan, longer-term droughts occur more frequently.

5. Atmospheric circulation changes associated with the interannual variation of drought and possible mechanisms

The standard deviations of seasonal precipitation are shown in the left column of Fig. 4. In every season, the precipitation standard deviation shows a decrease from southeast China to northwest China, with the largest variation over south China and the smallest variation over northwest China. The largest standard deviation of precipitation is seen in summer (Fig. 4e), with two centers [i.e., south China and the mei-yu/baiu/changma rainband region (28°–38°N, 105°–150°E)]. However, the variation of seasonal SPI shows a different pattern from precipitation. The largest variation of SPI is seen over northwest China in all seasons, with the center value exceeding 0.8. The SPI over north China also witnesses large variation, especially in spring and summer (Figs. 4d,f). Because both the features and the forcing mechanisms of the droughts in northwest China and the East Asian monsoon region are different, we review studies of droughts in these two regions separately in this section, with a focus on the year-by-year changes.

a. Drought in the East Asian monsoon region

The East Asian monsoon climate has complex spatiotemporal structures and shows distinct interannual variation modes. Seasonal drought in the East Asian monsoon region is dominated by the monsoonal circulation. The onset time of monsoon exerts an important influence on East Asian monsoon precipitation and temperature. If the onset of the summer monsoon is later and the duration is shorter, drought tends to occur in south China, the Yunnan Province, and north China, while severe flooding occurs in the Yangtze River and Huaihe River valleys (see Fig. 5 of Huang et al. 2007). Since summer rainfall accounts for 40%–50% (60%–70%) of the annual precipitation in south (north) China

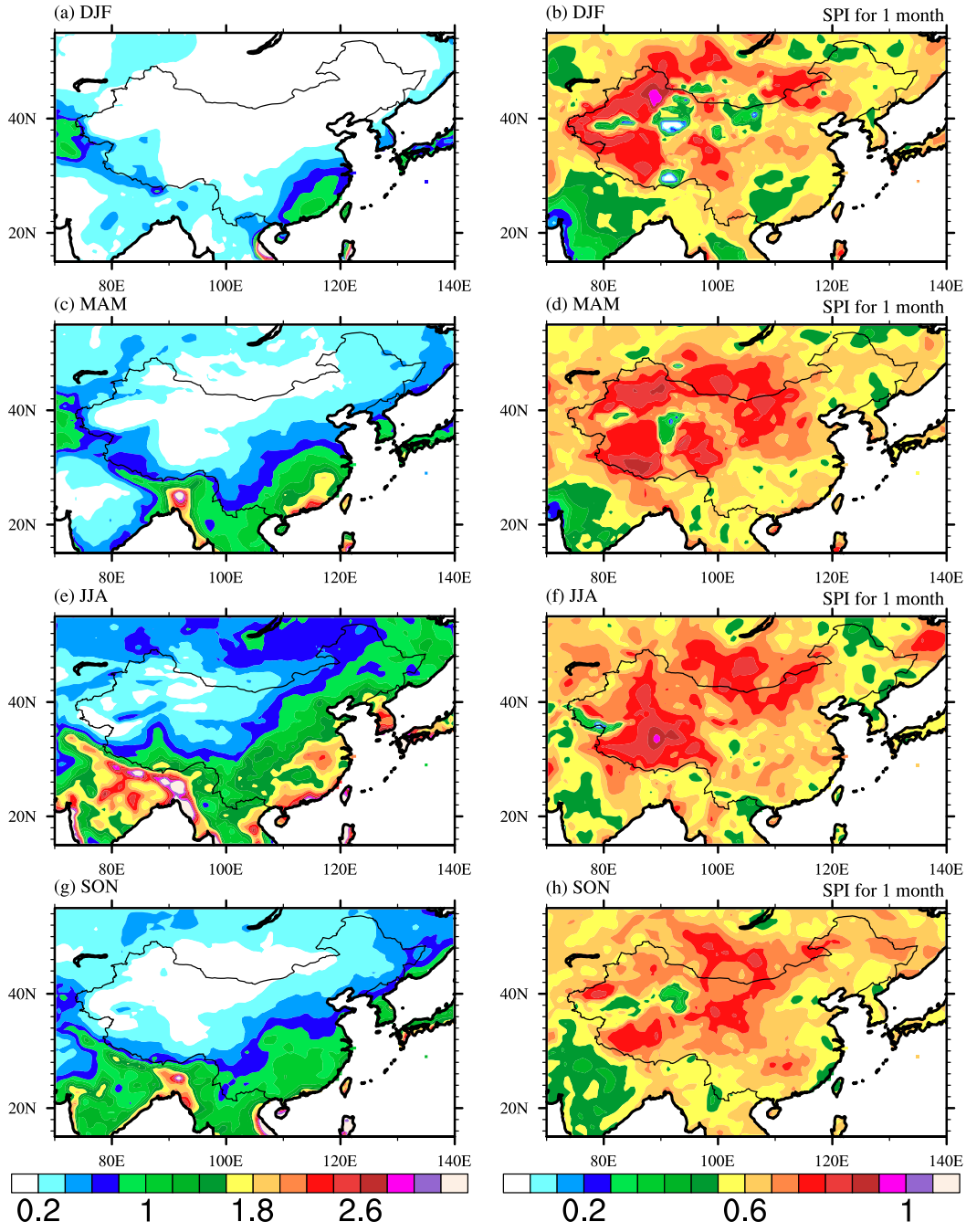

FIG. 4. (left) The distribution of the precipitation standard deviation (mm day^{-1}) during 1950–2009 in (a) DJF, (c) MAM, (e), JJA, and (g) SON. (right) As in (left), but for the seasonal mean SPI for a 1-month time scale. The precipitation and SPI-1 are both based on CRU.

(Gong 2007; Zhou et al. 2009a), drought activities in eastern China (east of 102.5°E) are dominated by the interannual variability of summer monsoon.

The East Asian summer monsoon is usually measured by an East Asian summer monsoon index (EASMI). The East Asian summer monsoon index proposed by Wang and Fan (1999) is used here. Its temporal variation and associated precipitation and circulation anomalies are shown in Fig. 5. Along with a strong East Asian monsoon, the interannual variability of eastern China summer precipitation features a meridional tripolar or sandwich pattern, with excessive precipitation in central-eastern China along the Yangtze River valley and Japan but drier or even drought conditions in southern and

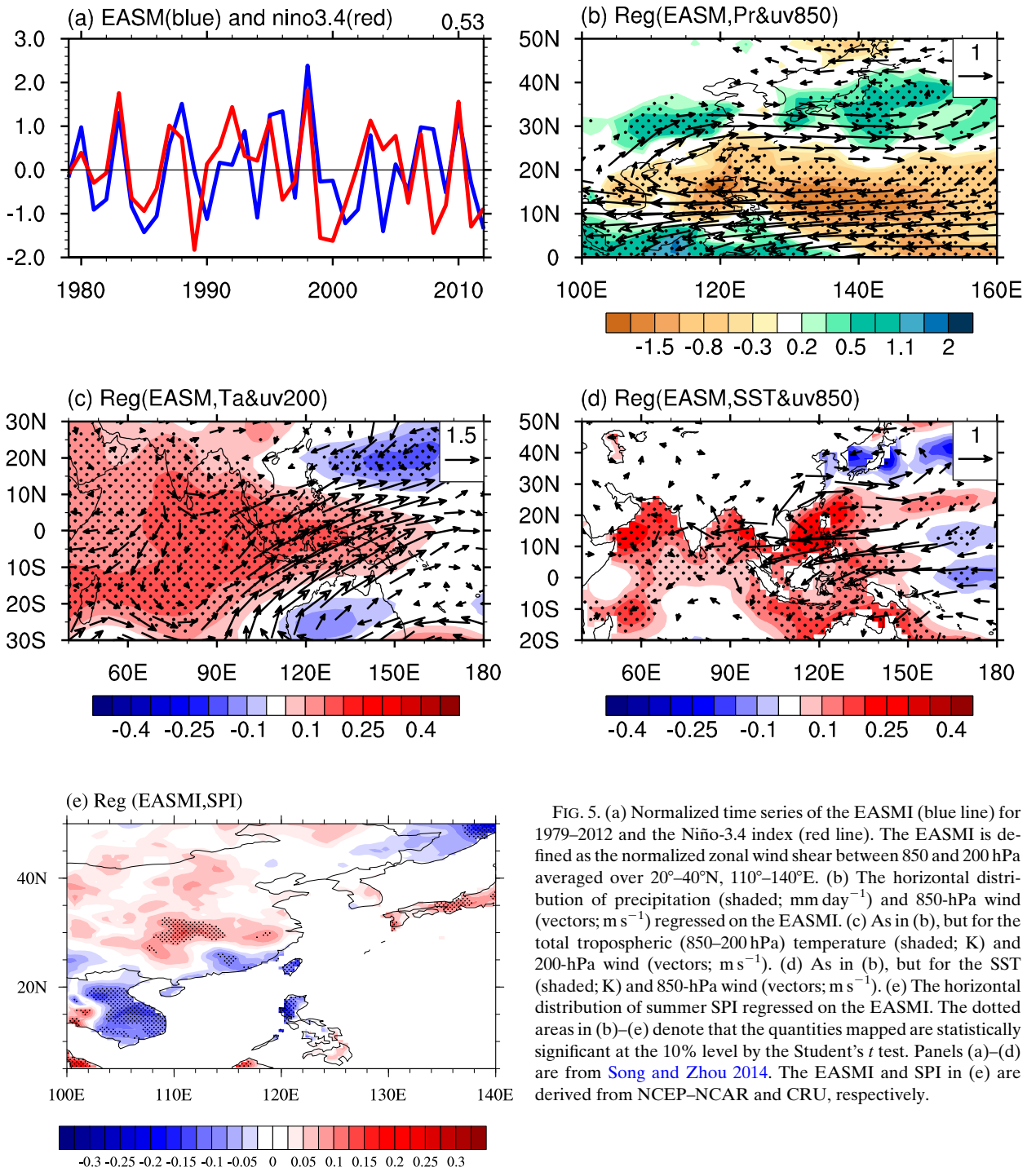

FIG. 5. (a) Normalized time series of the EASMI (blue line) for 1979–2012 and the Niño-3.4 index (red line). The EASMI is defined as the normalized zonal wind shear between 850 and 200 hPa averaged over 20°–40°N, 110°–140°E. (b) The horizontal distribution of precipitation (shaded; mm day^{-1}) and 850-hPa wind (vectors; m s^{-1}) regressed on the EASMI. (c) As in (b), but for the total tropospheric (850–200 hPa) temperature (shaded; K) and 200-hPa wind (vectors; m s^{-1}). (d) As in (b), but for the SST (shaded; K) and 850-hPa wind (vectors; m s^{-1}). (e) The horizontal distribution of summer SPI regressed on the EASMI. The dotted areas in (b)–(e) denote that the quantities mapped are statistically significant at the 10% level by the Student's *t* test. Panels (a)–(d) are from Song and Zhou 2014. The EASMI and SPI in (e) are derived from NCEP–NCAR and CRU, respectively.

northern China (Fig. 5b; Huang et al. 2012). The SPI anomaly (Fig. 5e) shows a similar pattern with that of precipitation, but only the correlation coefficient over the Yangtze River valley and Japan is statistically significant at the 5% level. Along with the tripolar precipitation pattern, a meridional Rossby wave train is seen along the East Asian coast, with an anomalous anticyclone appearing over the western North Pacific (WNPAC) north of 50°N and an anomalous cyclone from the Yangtze River valley to Japan (Fig. 5b). It is referred as the Pacific–Japan (PJ) or East Asian–Pacific teleconnection pattern (Nitta 1987; Huang et al. 2007). Increased southwesterly winds are seen over southeastern China and westerly along the Yangtze River valley and Japan, and they lead to excessive

precipitation from central China to southern Japan but drier conditions in southern China.

This wave train is forced by the anomalous heating over the western Pacific, especially near the Philippines, induced by anomalous precipitation associated with WNPAC (Li et al. 2008; Xie et al. 2009; Wu et al. 2009, 2010), which results from the atmospheric circulation changes driven by sea surface temperature anomalies associated with ENSO (Huang et al. 2007; Wu et al. 2009). The correlation coefficient between EASMI and the preceding winter Niño-3.4 index is 0.53 (Fig. 5a), statistically significant at the 95% confidence level. The corresponding SST anomalies and teleconnection are shown in Figs. 5c,d. An Indian Ocean basinwide warming is seen during El Niño decaying summer. It already exists in the El Niño mature winters and the subsequent spring but does not have a significant impact on anomalous circulation in the western North Pacific (WNP), because convection over the tropical Indian Ocean is suppressed by the remote forcing from the equatorial central-eastern Pacific. The basinwide warming plays an active role in impacting the WNPAC during ENSO decaying summers (Wu et al. 2009; Xie et al. 2009). The positive SST anomalies and associated precipitation anomalies over the Indian Ocean can warm the total troposphere and induce the upper-level circulation changes. Tropospheric warming emerges as a Matsuno–Gill (Matsuno 1966; Gill 1980) pattern with the heating anchored over the tropical Indian Ocean and exhibits a wedge penetrating into the WNP (Fig. 5c). Westerly winds dominate the equatorial Indo–western Pacific region, as the high-level Kelvin wave response of the Matsuno–Gill pattern, leading to an anomalous anticyclone over the WNP (Fig. 5d). A recent numerical modeling study demonstrates that the cold SST anomaly (SSTA) in the WNP is also active in maintaining the anomalous anticyclone. The negative SSTA in the WNP is crucial for the maintenance of the anticyclone in early summer, whereas in late summer, the Indian Ocean warming plays a more important role (Wu et al. 2010). In the following autumn, dry conditions appear over southeastern China. The anomalous precipitation pattern persists throughout the subsequent winter and spring (Wu et al. 2009). These kinds of observational patterns have been used as observational metrics to gauge the performances of climate models in simulating the interannual variability of the East Asian summer monsoon (Song and Zhou 2014).

Besides the PJ teleconnection pattern, another dominant teleconnection pattern is called the Silk Road pattern (Enomoto et al. 2003), which exerts significant influence on the East Asian monsoon climate. The Silk Road teleconnection is a teleconnection along the westerly jet stream in the upper troposphere over the Asian continent. Following Kosaka et al. (2012), the Silk Road pattern is identified by performing an EOF on 200-hPa meridional wind velocity over (30°–50°N, 30°–130°E) in summer. Both of the first two leading modes can be seen as a Silk Road pattern. Considering the robust correlation with the East Asian summer rainfall, only the first leading mode (EOF1) and the corresponding principal component (PC1) are shown in Figs. 6a,b. The fractional variance explained by the EOF1 is 39.8% and can well separate from other modes based on the north's criteria (North et al. 1982). The Silk Road pattern features a wave train structure along the Asian jet (Fig. 6a), with four centers located near 40°, 65°, 95°, and 130°E. The center near 130°E in EOF1 was associated with the Bonin high, as discussed by Enomoto et al. (2003). The wave activity flux propagated eastward along the Asian jet east of 60°E and finally moved southward again to the exit of the jet (Fig. 6a). The flux indicates that the eastward-propagating wave train originated from the North Sea and the Caspian Sea (Sato and Takahashi 2006). Associated with the Silk Road teleconnection, a significant enhancement of precipitation is seen over north China, but significant deficient rainfall dominates over South Korea and Japan (Fig. 6c). The distribution of drought is consistent with that of precipitation anomalies (Fig. 6d), which indicates that the summer drought over north China is mainly caused by the precipitation deficient.

Most studies documented that the Silk Road teleconnection is forced by Indian monsoon heating and is a propagation of stationary Rossby waves along the Asian jet in the upper troposphere (Wu et al. 2003; Wu et al. 2003). We can see significant increased rainfall over the Indian monsoon region in Fig. 6c. Ding and Wang (2005) showed that the Silk Road pattern is a regional manifestation of a circumglobal teleconnection (CGT) that is recurrent in the Northern Hemispheric summer. The CGT pattern is closely associated with Indian summer monsoon (ISM) variability and may also be indirectly influenced by ENSO during periods of strong interactions between ISM and ENSO. Ding et al. (2011) further found that CGT appears preferentially in summers preceding the peak phases of the cycle when an ISM precipitation anomaly is evident. During ENSO developing summer, for instance the El Niño years, the warm SST anomaly has attained a certain magnitude in the eastern Pacific; this warm SST anomaly, through the equatorial anomalous heating, may induce subsidence anomalies over the Maritime Continent, which further suppresses the ISM through the Rossby wave response to the suppressed convection over the Maritime Continent (Wang et al. 2003). Ding and Wang (2005) showed that the ISM acts as a ''conductor'' connecting the CGT

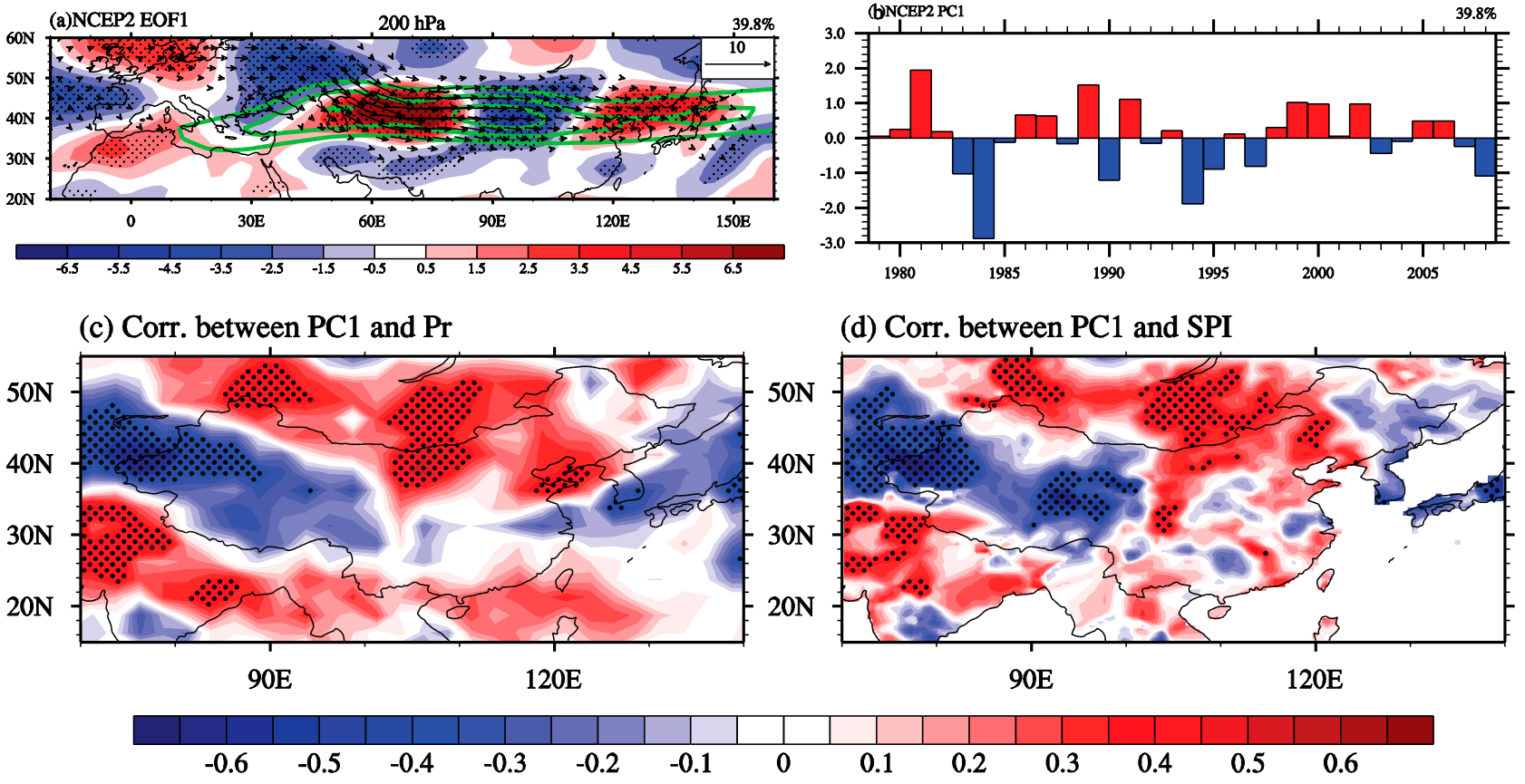

FIG. 6. (a) Vorticity anomalies ($10^6\,s^{-1}$; shading) at 200 hPa regressed onto PC1 of the 200-hPa meridional wind velocity over (30°–50°N, 30°–130°E) in JJA derived from the NCEP–DOE reanalysis. The regression coefficients that are statistically significant at the 5% level are dotted. Green contours show climatological zonal wind velocity $>20\,m\,s^{-1}$. Arrows represent the wave activity flux ($m^2\,s^{-2}$; according to Takaya and Nakamura 2001) calculated with regressed anomalies. The variance fraction explained by EOF1 is denoted near the upper-right corner. (b) The standardized PC1 of 200-hPa meridional wind velocity over (30°–50°N, 30°–130°E) in JJA. (c) Correlation coefficient between precipitation (based on GPCP) and PC1. The dotted areas are statistically significant at the 5% level. (d) As in (c), but for summer SPI and PC1. Panels (a),(b) are from Song and Zhou 2013).

and ENSO. When the interaction between the ISM and ENSO is active, ENSO may influence north China via the ISM and the CGT. This mechanism explains why the drought in India has been in phase with that in north China (Guo 1992; Wu et al. 2003; Liu and Ding 2008).

The impact of ENSO on eastern Asian drought activities exhibits interdecadal variability. Since the late 1970s, the overall coupling between the East Asian system and the ENSO has become strengthened (Wang et al. 2008). Pre-1979, El Niño events dissipated more quickly than those that occurred post-1979. Since the late 1970s, the warming in the equatorial eastern Pacific has been able to persist from boreal winter to the following spring and even the summer, leading to an enhanced delayed relationship between the East Asian monsoon and ENSO. Thus, more droughts tend to occur in southern China in years involving an El Niño decaying summer (Wang et al. 2008).

In addition to the above-mentioned two teleconnection patterns forced by tropical SST anomalies, some other factors, such as the North Atlantic Oscillation (NAO) and the thermal condition of the Tibetan Plateau, are also regarded as possible impacting factors of East Asian drought. In winter, the NAO can modulate the extratropical atmospheric circulation system (Siberian high and East Asian jet stream) to influence the variability of East Asian precipitation (Z. Wang and Y. Ding 2006; Mao et al. 2007). Gong and Ho (2003) also documented that a positive NAO in late spring could lead to a northward shift of the East Asian summer jet stream and change the precipitation over the Yangtze River valley. Xin et al. (2010) suggested that the increased Tibetan Plateau snow depth is an indicator of the connection between enhanced winter NAO and late-spring tropospheric cooling over East Asia. The late spring tropospheric cooling over East Asia further led to a drought over southern China (Xin et al. 2006). Zhang et al. (2003) found the existence of a close relationship between the interdecadal increase of snow depth over the Tibetan Plateau during the preceding spring and the excessive summer rainfall over Yangtze River basin. Ding and Sun (2003) proposed that the excessive snow results in a decrease in heat sources over the Tibetan Plateau, through the increased albedo and spring snow melting, thus reducing the land–sea thermal contrast, the driving force of the Asian summer monsoon. For a specific drought event, the influences of individual factors might be different. The severe drought of 2010/11 may be attributed to the combined effects of La Niña, a positive phase of NAO, and the weak thermal condition of the Tibetan Plateau (Sun and Yang 2012). Therefore, the formation of drought is quite complicated.

b. *Drought over NW China*

NW China is located at the inland of the Eurasian continent and is far away from the surrounding oceans. Precipitable water in summer is only ½–⅓ of that in the East Asian monsoon region. Ye and Gao (1979) and Xu and Zhang (1983) were the first to describe the thermal and dynamical impact of the Tibetan Plateau (TP) on the formation of the climate of NW China. First of all, the high topography of the TP blocks the warm and wet air from southwest to NW China. Second, the TP is a heat source relative to the surrounding regions. In summer, an upward motion dominates the TP and leads to compensative descending motion over NW China. In the upper troposphere, a southerly wind moves northward from the TP, while in the midtroposphere (500 hPa) a northerly wind moves back to the TP (Wu and Qian 1996; Qian and Zhu 2001). The long persistence of these circulations results in a deficiency of rainfall in the region. This is the climatological drought background of NW China (Zhang et al. 2009).

On the interannual time scale, drought is associated with the prevailing anomalous circulation. Wu and Qian (1996) examined the circulation in wet and dry summers of NW China and documented that these circulation anomalies are caused by the anomalous surface heating of the TP. We replotted the circulation anomalies for wet and dry years of NW China using recent data. As in Wu and Qian (1996), the wet (dry) years are 1979, 1981, and 1983 (1980, 1985, and 1986). The precipitation and circulation distribution in wet and dry years of NW China is shown in Fig. 7. In wet years (Fig. 7a), the South Asian high at 100 hPa shifts more east than that in dry years, the midtroposphere is dominated by an anomalous cyclone, and the westerly jet at 200 hPa north of the TP is weaker than that in dry years. This is beneficial for upward motion over the north of the TP (Fig. 7c) and, thereby, excessive rainfall over NW China. In contrast, for dry years (Fig. 7b), the South Asian high is located west of 100°E, the 500-hPa circulation is dominated by an anomalous anticyclone over NW China, and the westerly jet at 200 hPa over the north of the TP is stronger. The above circulation would weaken the upward motion over the TP but enhance descending motion over NW China, leading to a deficiency of rainfall in the region (Fig. 7d; Wu and Qian 1996). The majority of TP (25°–40°N, 70°–100°E) is dominated by anomalous upward motion in wet years but descending motion in dry years. They documented that the circulation anomalies are related with the heating of the TP. In wet years, the heating of the TP is larger than normal, and the heating effect of the TP is intensified, while it is weaker than normal in dry years. The impact of the TP on the

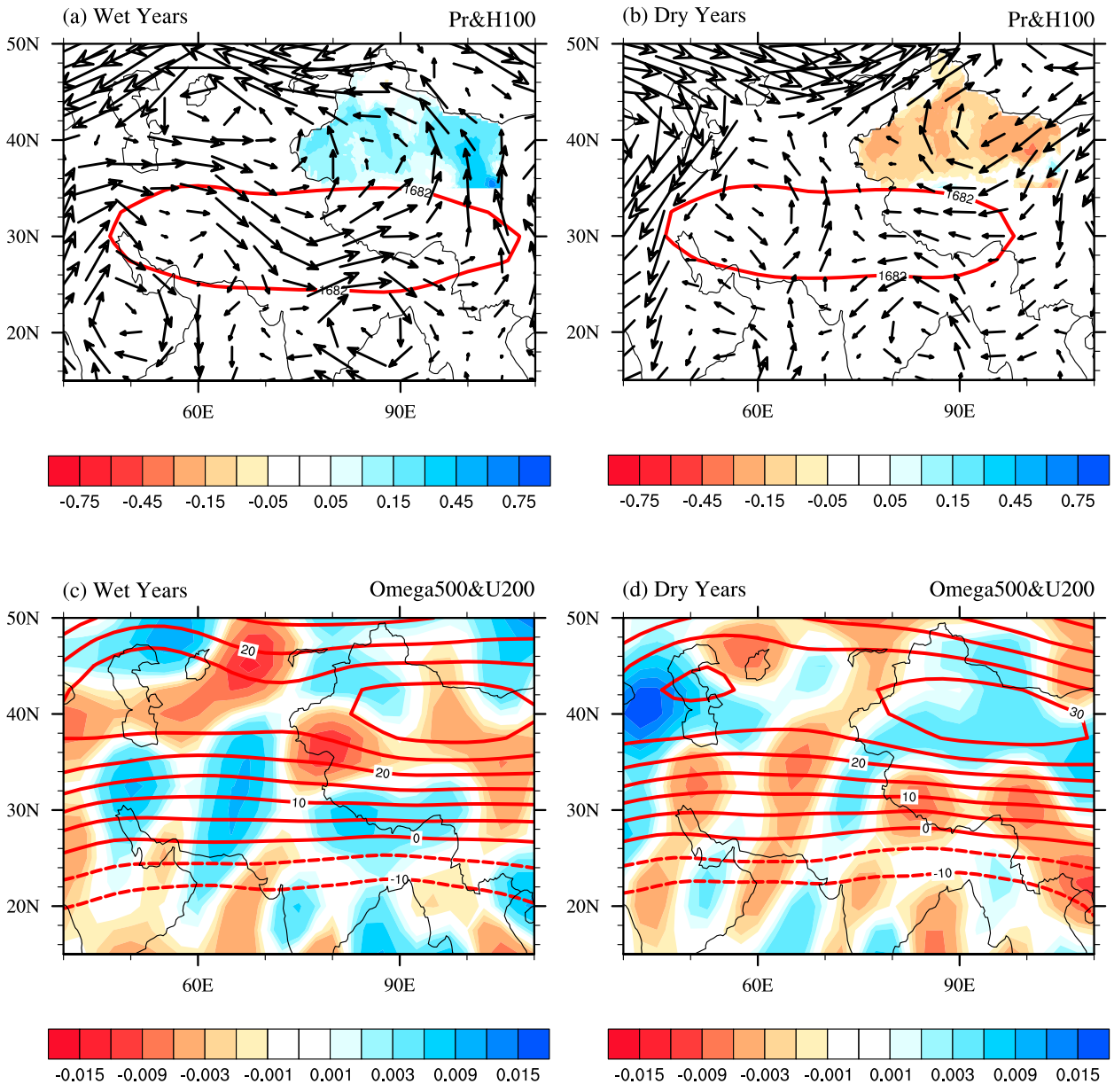

FIG. 7. The distribution of geopotential height at 100 hPa (contours; 10 × gpm) and anomalous precipitation (shaded; mm day^{-1}) and wind at 500 hPa (vectors; m s^{-1}) for (a) wet years and (b) dry years. Only the precipitation anomalies over NW China and at 16 820 gpm (standing for the location of the South Asian high) are shown. (c),(d) The distribution of zonal wind at 200 hPa (contours; m s^{-1}) and anomalous vertical velocity at 500 hPa (shaded; pa s^{-1}) in wet years and dry years, respectively. The selected period is 1979–90, and the wet and dry years are as in Wu and Qian (1996). The atmospheric circulations and precipitation anomalies are based on NCEP–NCAR and CRU, respectively.

atmospheric hydrological cycle and thermodynamic effects was verified by Fan and Cheng (2003a,b) using a climate model.

Besides the heating of the TP, many other factors might affect drought in NW China. For instance, the snow depth of the TP (Wu et al. 1998), the summer Arctic Oscillation (AO) (P. Wang et al. 2007), and ENSO (Li and Li 2004). When the summer AO is weaker, a cyclonic anomaly appears in Baikal and its southern region at 700 hPa, with an anomalous westerly wind over NW China. The enhanced westerly wind is conducive to more rainfall over NW China (P. Wang et al. 2007). During El Niño developing years, rainfall is deficient, and temperatures are high over most areas of NW China, but low temperatures and more rain dominate the Xinjiang Province (35°–50°N, 75°–95°E). In the

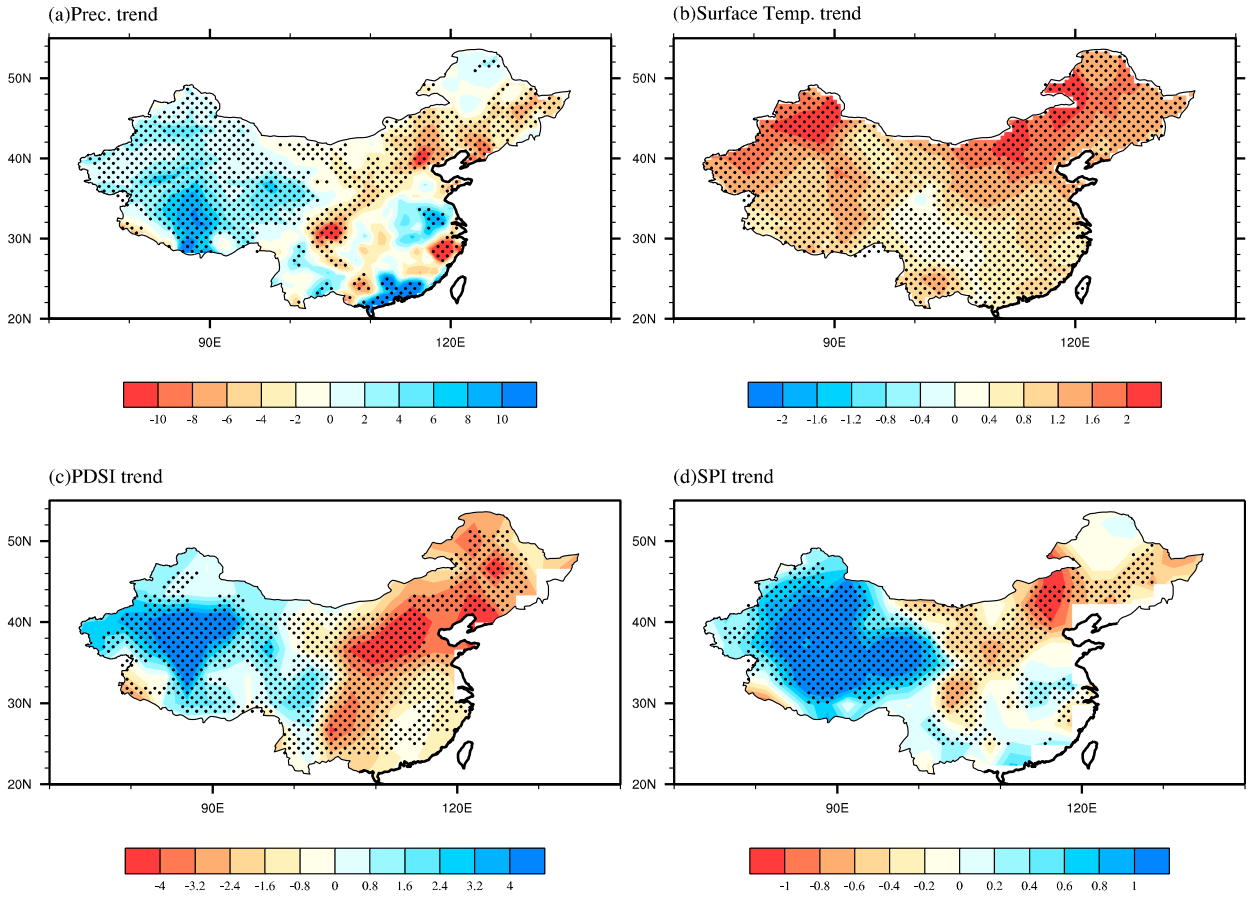

FIG. 8. Linear trend for annual mean (a) precipitation [mm day^{-1} (50 yr)$^{-1}$], (b) surface temperature [°C (50 yr) $^{-1}$], (c) sc-PDSI, and (d) SPI-12 during 1950–2009 [units: (50 yr)$^{-1}$]. The dotted areas are statistically significant at the 10% level.

years following El Niño years, Xinjiang and the east side of the Qinghai–Xizang Plateau are wetter and colder than normal (Li and Li 2004).

Since NW China is an arid/semiarid region, it is more sensitive to drought disasters. Although many studies have noticed the relationship between drought in NW China and the two types of oscillation (ENSO and AO), they have done so based largely on statistical analyses; the underlying mechanisms remain unclear.

6. Long-term trend of drought severity and extent over East Asia

a. Observational evidence for the long-term trend of drought

Drought trends have been well documented by many works in terms of drought occurrence, area, and intensity. For example, by examining the dryness and wetness trends for the period 1470–1999 derived from Chinese historical documents and instrumental observations, Qian et al. (2003) showed that the frequency of severe dryness and severe wetness has increased in eastern China since the early twentieth century, coinciding with recent global warming. Qian and Zhu (2001) analyzed the droughts of seven regions over China from 1880 to 1998, and found that the aridification trend has become more serious since the 1970s in north China, and drought in north China reached a high during the 1990s; while along the Yangtze River valley, drought mainly appeared from the 1920s to early 1940s. Qiu et al. (2013) showed that the cumulative frequency and grain loss has a good power-law relationship in China for the period 1950–2010.

More attention has been paid to the changes in drought in the second half of the twentieth century. The linear trends of sc-PDSI and SPI-12 for 1950–2010 are shown in Fig. 8. Both sc-PDSI and SPI-12 show a zonal dipole pattern, with an increasing trend over NW China but a decreasing tendency over north China for 1950–2010 (Figs. 8c,d). The latter is usually termed the north China drought. It is identified by many studies using precipitation (Xu 2001; Zhou et al. 2009a), soil moisture index (Ma and Fu 2006), and some other drought indices. The north China drought is mainly caused by

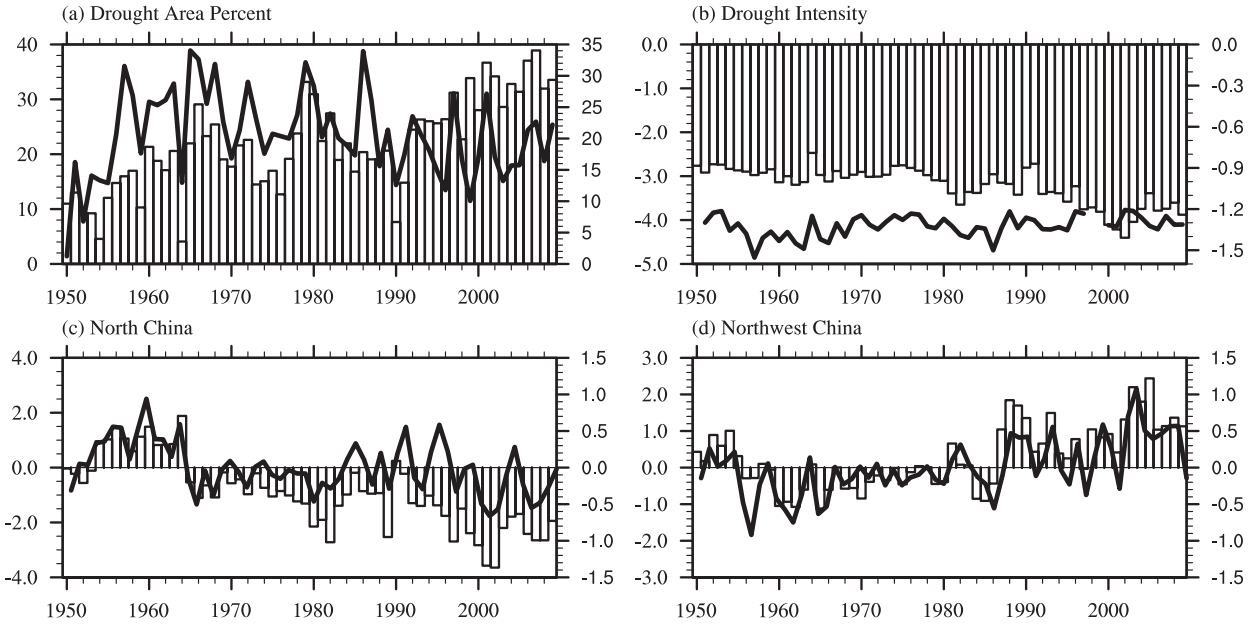

FIG. 9. The time series of (a) drought area percentage (%) for 1950–2009 over China derived from sc-PDSI (bars) and SPI-12 (line). The drought area is defined as the region where sc-PDSI < -2.0 and SPI-12 < -0.8. (b) As in (a), but for drought intensity, which is averaged sc-PDSI (SPI-12 < -0.8) over the areas where sc-PDSI < -2.0 (SPI-12 < -0.8). (c),(d) The annual variation of sc-PDSI (bars) and SPI-12 (line) over north China (35°–55°N, 105°–130°E) and northwest China (30°–55°N, 70°–105°E), respectively. The left *y* axis is for sc-PDSI, and the right *y* axis is for SPI-12.

decreased precipitation and intensified by increasing temperature (Figs. 8a,b).

The drought area percentage and drought intensity changes for 1950–2010 are shown in Fig. 9. A significant increasing trend of sc-PDSI is observed in drought area (PDSI < -2). Both the drought area and drought intensity have enhanced in the past 60 years. However, the drought area and intensity shows no significant trend in SPI-12. The difference may be because the SPI only contains the impact of precipitation, which shows opposite trends over northwest and south China (Fig. 8a), leading to no trend by averaging over China. The annual variation of sc-PDSI and SPI-12 over north China and NW China are shown in Figs. 9c,d. A significant increasing drought tendency can be seen from both sc-PDSI and SPI-12 for north China, with a stronger magnitude for sc-PDSI. In contrast, both sc-PDSI and SPI-12 show increasing trends over NW from 1950 to 2005 with a phase transition around the late 1980s, which indicates that the drought condition of NW China gets relieved. For PDSI averaged over the whole of continental China, there is no significant long-term trend in the percentage areas of drought (defined as PDSI < -1.0) over the period 1951–2003 (Zou et al. 2005). This is because we used sc-PDSI in this work, and the drought area is defined as PDSI < -2.0; while they used PDSI, and the drought area was defined as PDSI < -1.0. Wang et al. (2011) also found no significant trend in China over 1950–2006 based on soil moisture. However, severe and prolonged dry periods since the late 1950s are seen in most parts of north China regardless of what kind of indices are used. The increased drought in north China has induced severe environmental problems, such as no flow in the lower reaches of the Yellow River and the salinization of soil in north China (Qian and Zhu 2001).

Many studies documented that NW China—most notably in Xinjiang Province—has shifted from a warm/dry climate to a warm/wet climate since 1987 (Figs. 8c,d; Ma and Fu 2006; Shi et al. 2007). The change in drought occurrence is also reflected in other meteorological elements (e.g., increased air temperature and precipitation, melting of glaciers, increased glacial meltwater and river runoff, and raised water levels of inland lakes) compared with the climatological mean of 1961–86 (Shi et al. 2007). However, the relative increase in precipitation cannot change the arid/subarid climate there, since the total amount of precipitation is still limited (Ma and Fu 2006). A recent study found that the severity and spatial extent of aridity and drought have increased substantially in northwestern China in the past 10 years because of an increase in evaporation resulting from the continuous rise in temperature (Wei and Wang 2013).

b. *Mechanisms for the drought trend over East Asian monsoon regions*

The drying trend over north China in the second half of the twentieth century is associated with a persistent warming and less precipitation (Figs. 8a,b). A shift from wet to dry conditions in north China can be seen from the mid and late 1970s to the present (Ma 2007). This transition is related to the interdecadal scale weakening of the East Asian summer monsoon (EASM) circulation. The EASMI for 1950–2009 are shown in Fig. 10a, with a decreasing trend [$-1.82\ (50\,\mathrm{yr})^{-1}$] statistically significant at the 5% level. There is a phase shift of EASMI around the late 1970s. The increasing drought in north China is a regional manifestation of this long-term or interdecadal change of precipitation associated with monsoon activities. The precipitation and circulation difference between the 1978–2009 and 1950–77 are shown in Fig. 10b. The associated precipitation changes appear as deficient rainfall in north China but excessive rainfall in the Yangtze River valley along 30°N, and this kind of precipitation pattern is known as the "south flood–north drought" pattern in China (Fig. 10b; Hu 1997; Wang 2001; Gong and Ho 2003; Yu et al. 2004; Yu and Zhou 2007). Significantly anomalous northerly winds are seen along East Asia (Fig. 10b), leading to less northward transport of tropical water vapor to north China, but more water vapor converges over the Yangtze River valley. This results in increased moisture convergence and excessive rainfall in the south and deficient rainfall in north China.

Although there is debate regarding the mechanisms responsible for the observed monsoon weakening [see Zhou et al. (2009a) for a review], there is increasing evidence demonstrating that the weakening tendency of summer monsoon circulation and the associated increasing tendency of drought in north China are part of global land monsoon changes (B. Wang and Q. Ding 2006; Zhou et al. 2008b; Zhang and Zhou 2011). The global land monsoon precipitation has experienced a declining trend during the second half of the twentieth century (B. Wang and Q. Ding 2006). This trend is actually an interdecadal variability driven by the phase transition of the Pacific decadal oscillation (PDO) (Zhou et al. 2008a, 2013). The phase transition of PDO changed from negative to positive phase around the end of 1970s (Fig. 10a). The correlation between the observed EASMI and PDO is 0.62, statistically significant at the 5% level. Furthermore, the EASMI trend can be well simulated by the Community Atmosphere Model, version 3.0 (CAM3.0), forced by historical SST (Fig. 10a; Li et al. 2010). From the correlation coefficients between EASMI and SST both in observation and simulation (Figs. 10c,d), we can see significant negative correlations of 0.5–0.7

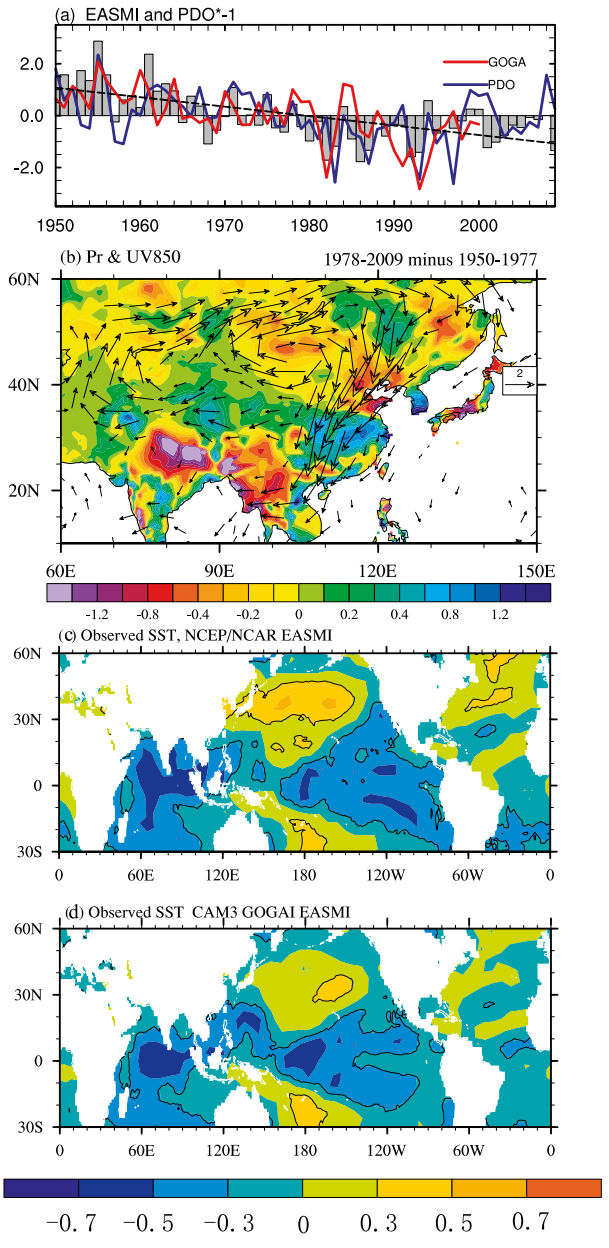

FIG. 10. Time series of EASMI (bars) and its trend (dashed line) from the NCEP–NCAR reanalysis for 1950–2009, the PDO index (multiplied by −1; blue line), and the EASMI derived from a simulation of CAM3.0 forced by observed monthly SSTs over the global oceans from 1950 to 2000 (red line). (b) Difference of precipitation (shaded; mm day^{-1}; derived from CRU) and wind at 850 hPa (vectors; m s^{-1}; only values that are statistically significant at the 5% level are shown, derived from NCEP–NCAR) between 1978–2009 and 1950–77. (c),(d) The correlation coefficient between observed JJA SST at each grid box and the EASMI from the NCEP–NCAR reanalysis and CAM3.0, respectively. Panels (a),(b) are as in Li et al. 2010, but extended to 2009. Panels (c),(d) are from Li et al. (2010). The PDO index is downloaded from the JISAO website (http://jisao.washington.edu/pdo/PDO.latest).

over the tropical central and eastern Pacific and central Indian Ocean, while positive correlations exist over the North and South Pacific. The phase transition of PDO has led to a weakened land–sea thermal contrast and thereby a weakened EASM circulation (Li et al. 2010), followed by an increasing drought tendency in north China.

The forcing of PDO to the EASM circulation and thereby drought activities is more evident if we extend our analysis to the changes of drought during the whole of the twentieth century. Qian and Zhou (2014) examined the dry–wet changes in north China during 1900–2010 on the basis of self-calibrated PDSI data. The ensemble empirical mode decomposition method was used to detect multidecadal variability. They highlighted that approximately 70% of the drying trend during 1960–90 originated from 50–70-yr multidecadal variability related to PDO phase changes. The PDSI in north China is significantly negatively correlated with the PDO index, particularly at the 50–70-yr time scale. This negative correlation relationship is stable during 1900–2010 (Qian and Zhou 2014).

In addition to the natural forcing of PDO, the TP thermal forcing (Duan and Wu 2008) and anthropogenic forcing agents including aerosols (Menon et al. 2002; Wang et al. 2013) have also been suggested as mechanisms that have driven the long-term monsoon and thereby drought changes over East Asia. A regional model study on land-use effects showed that the land use modified by anthropogenic activities may result in a reduction of precipitation and an increase of temperature over north China (Gao et al. 2007). A recent analysis of 17 models from phase 5 of the Coupled Model Intercomparison Project (CMIP5) found that, although the aerosol forcing can drive a weakened monsoon circulation in the model experiments, the models' responses are far weaker than the observation. The models fail to reproduce the observed precipitation changes, including the drought trend in north China (Song et al. 2014). They suggest that the internal variability mode of the PDO has played a dominant role in the monsoon weakening, while the aerosol forcing plays a secondary or complementary role. The emission of greenhouse gases favors an enhanced monsoon circulation, but the model response is weaker than that of aerosols.

In summary, the increasing drought in north China in the second half of the twentieth century is consistent with the weakening tendency of EASM circulation. The monsoon weakening is a regional manifestation of global land monsoon changes driven by the phase transition of the PDO (Zhou et al. 2013). Thus, natural variability is the dominant factor that determines the long-term drought changes in north China. Simulation experiments using CAM3.0 demonstrate that greenhouse gases plus aerosol forcing (direct effect) increases the land–sea thermal contrast and thus enhances the EASM circulation (Li et al. 2010), which will lead to excessive rainfall in north China. Recent studies have also reported a recovery of EASM circulation in the present century (Zhu et al. 2011; Liu et al. 2012; Lin et al. 2014), and whether or not this indicates drought in north China is weakening deserves further study.

7. Prediction and projection of drought in China

a. Studies on drought prediction

The prediction of the East Asian monsoon is a topic with a long history and is still of concern today both in the scientific research community and operational forecasting groups. The prediction over East Asia mostly concentrates on precipitation. SST-constrained Atmospheric Model Intercomparison Project (AMIP)-type atmospheric general circulation model (AGCM) simulations show low skill in predicting East Asian monsoon precipitation, including its climatological position, annual cycle, and interannual variation (Chen et al. 2010; Zhou et al. 2009b; Li et al. 2010; Li and Zhou 2011). The recent work by Sperber et al. (2013) showed that the climate models that participated in CMIP5 show better performance in simulating East Asian monsoon circulation and precipitation but still cannot satisfactorily reproduce its onset and retreat. Song and Zhou (2014) investigated the interannual variability of EASM simulated by AGCMs in phase 3 of CMIP (CMIP3) and CMIP5, and found that the rainband known as mei-yu/baiu/changma (28°–38°N, 105°–150°E) is poorly simulated, although significant improvement is seen from CMIP3 to CMIP5. The interannual EASM pattern is partly reproduced in the CMIP3 and CMIP5 multimodel ensemble (MME), but with weaker magnitude and a southward shift of the dipole rainfall pattern. They documented that a successful reproduction of interannual EASM pattern depends highly on the Indian Ocean–western Pacific anticyclone teleconnection. This provides lights to the prediction of droughts in the East Asian monsoon area.

Dynamic seasonal forecasting systems based on coupled atmosphere–ocean–land general circulation models (CGCMs) have been widely used for drought prediction in recent years (Luo and Wood 2007; Dutra et al. 2013; Yuan and Wood 2013). Kang et al. (2004) showed that extratropical precipitation is less predictable than in the tropics because of the large contribution of internal atmospheric processes. Their work was based on the seasonal prediction experiment of the Climate and Ocean: Variability, Predictability and Change (CLIVAR) Seasonal Prediction Model Intercomparison Project II (SMIP II). High forecasting skill of surface temperature

and precipitation is mostly seen in the tropics, while it is almost zero in East Asia, as derived from the Asia–Pacific Economic Cooperation (APEC) Climate Center (APCC)/Climate Prediction and its Application to Society (CliPAS) hindcast results (Wang et al. 2009). The poor prediction of East Asian monsoon precipitation is also seen in the seasonal forecasts of ECMWF System 4 and NCEP Climate Forecast System, version 2 (CFSv2), and the DEMETER project (Kim et al. 2012; Kang et al. 2004; Luo et al. 2013; Yang et al. 2008; Liu et al. 2014). The seasonal hindcast results of the APCC/CliPAS and DEMETER projects can satisfactorily predict the four observed EOF modes of Asian winter temperature variability, which are related with ENSO and AO (Lee et al. 2013). Using 28-yr (1982–2009) North American Multimodel Ensemble (NMME) hindcast data with 110 ensemble members, Yuan and Wood (2013) found that the multimodal ensemble increases the drought detectability over some tropical areas where individual models have better performance but cannot help over most extratropical regions, such as East Asia.

Although the precipitation of East Asia is poorly predicted, the climatological and interannual variation of circulation can be reproduced well by climate models. Yang et al. (2008) showed that the NCEP Climate Forecast System (CFS) can successfully predict the major dynamical monsoon indices and monsoon precipitation patterns several months in advance, and the skill mainly derives from the impact of ENSO. Kim et al. (2012) pointed out that the Asian monsoon appears to be well predicted during years with strong ENSO forcing. The two dominant teleconnections that influence East Asia [i.e., the Pacific–Japan pattern (Nitta 1987) and the Silk Road pattern (Xiao et al. 2009; Kosaka and Nakamura 2006)] are key factors for East Asian climate prediction. The former is associated with ENSO and can generally be captured by climate models, while the latter cannot be predicted because of its lack of correlation with ENSO. Zhou and Zou (2010) examined the reason for the predictability of EASM from the reproduction of land–sea thermal contrast change in AMIP-type simulations and found that the prediction skill mainly comes from the predictability of the meridional land–sea thermal contrast. Through comparing two ensembles of AGCM simulations forced with observed monthly SST and their climatological annual cycle, Ferguson et al. (2010) investigated the influence of SST forcing on stochastic characteristics of simulated seasonal precipitation and drought. They showed that SST anomalies have no significant influence on simulated drought frequency, duration, and magnitude over East Asia, and severe and sustained drought events may occur in the absence of persistent SST forcing.

Two principle reasons are responsible for the poor level of skill in simulating EASM by AGCMs: one is that many defects still exist in the physical processes of these models, and the other is that air–sea interaction is not taken into consideration in SST-forced AGCM simulations (Wu and Kirtman 2005, 2007; Wang et al. 2005). In contrast to studies of precipitation and atmospheric circulation, less effort has been devoted to the seasonal prediction of East Asian drought. In addition, most attention is paid to the East Asian monsoon region, while examinations of NW China are few in number. Therefore, a systematic examination of drought simulation and prediction is needed. In particular, an intensive analysis of drought in NW China should be carried out.

b. Projection of future changes in drought

Previous studies have indicated that global warming might contribute to more frequent and severe drought. It is crucial to study the impact of warming related to greenhouse gases on East Asian drought by comparing projected climates. Kim and Byun (2009) investigated the drought pattern based on the simulations of 15 coupled climate models under the SRES A1B scenario. They found that Asian monsoon regions show a greater increase in the standard deviation of precipitation than the mean precipitation, with an amplified seasonal cycle of precipitation, which results in a slight increase in drought frequency and intensity over parts of the Asian monsoon regions. Simulations by RegCM2 nested with a CSIRO model indicate that the warm/wet climate over NW China will continue under a doubling of CO_2, but aerosols and natural factors might reduce this increase of magnitude (Shi et al. 2007).

Using the Hadley Centre climate model under the SRES A2 scenario, Burke et al. (2006) examined the projected global drought for the twenty-first century and found a drying tendency over eastern Asia. Sheffield and Wood (2008) investigated the projected changes of drought occurrence under future global warming in multimodel, multiscenario IPCC AR4 simulations, and found that the models show decreases in soil moisture globally under all scenarios with a corresponding doubling of the spatial extent of severe soil moisture deficits and frequency of short-term (4–6-month duration) droughts from the mid-twentieth century to the end of the twenty-first century. Nevertheless, the changes over East Asia are predicted to be relatively small. The PDSI change projected by 22 CMIP3 climate models under the SRES A1B scenario (Dai 2011a) exhibits an increasing trend of drought in Southeast Asia. Zhou and Hong (2013) compared the potential change of global drought using PDSI with two potential evapotranspiration equations using a coupled climate system model

(FGOALS-s2) under the representative concentration pathway 8.5 (RCP8.5) scenario. They found that the algorithm of the Thornthwaite equation overestimates the impact of surface temperature on evaporation and leads to an unrealistic increasing of drought frequency, while the algorithm based on the Penman–Monteith equation is physically reasonable and necessary for climate change projections. This model projects an increasing trend of drought during 2051–2100 in Southeast Asia under the RCP8.5 scenario. The 14-model ensemble mean from CMIP5 also projects an increasing trend in Southeast Asia (Dai 2013), similar to the changes simulated by FGOALS-s2. Sillman et al. (2013) analyzed global changes in the consecutive dry-day (CDD) index over the twenty-first century relative to the reference period 1981–2000 using the CMIP5 multimodel ensemble under different emission scenarios. They showed that CDD increases in Southeast Asia, which is combined with increases in the heavy precipitation days index (R10mm) and maximum 5-day precipitation index, indicating an intensification of both wet and dry seasons in this region. Using two ensembles from the Hadley Centre AGCM and other AGCM 2 × CO_2 equilibrium runs, Burke and Brown (2008) computed four different drought indices and found that in Indochina the sign and magnitude of the change in drought is dependent on index definition and ensemble number.

The above analysis shows that, under the SRES A1B scenario and doubled CO_2 simulations, most climate models project an increasing drought frequency and intensity based on soil moisture, PDSI, and precipitation. However, the projection pattern and severity depend on the climate model and drought index. Burke and Brown (2008) pointed out that it is only those regions where there is a consistent increase in drought across all indices and ensembles where the annual average precipitation decreases. East Asia is covered by different climate zones, and the precipitation changes show distinct regional characteristics. Therefore, the selection of appropriate indices is important for drought impact studies.

8. Summary

In this paper, we reviewed the occurrence and known areas of severe drought, the atmospheric circulation and potential mechanisms that impact the interannual variation of drought, and the long-term trend and associated mechanisms, predictability, and projection of East Asian drought. The following is the synthesis of the above aspects of East Asian drought:

1) Drought events that occurred over the past 100 years can be clustered into several periods. During 1950–2010, the major drought periods of China occurred in 1959–61, 1978–82, 1987–94, and 1997–2002. The main drought events in China and the associated impacts are described in this paper, and a summary can be found in Table 2.
2) Dominated by the monsoonal circulation, drought over East Asia shows apparent seasonal variation. The seasonal drought over the East Asian monsoon region is closely related with the onset, duration, and ending of monsoon circulation. In spring, drought mostly occurs over north China and southwest China. North China and southwest China are the regions with the highest drought frequency and maximum duration areas.
3) The circulation and possible mechanisms responsible for the interannual variation of East Asian drought were discussed. The drought in eastern China, Japan, and the Korea Peninsula is dominated by the East Asian monsoon variability. There are two teleconnections that dominant the interannual variability of eastern China's summer precipitation. One is the Pacific–Japan (PJ) or East Asian–Pacific teleconnection pattern. The precipitation anomaly features a meridional tripolar or sandwich pattern, with excessive precipitation in central-eastern China along the Yangtze River valley and Japan but drier or even drought conditions in southern and northern China. It is forced by an anomalous anticyclone that appears over the WNP, which is forced by the SST anomalies over the WNP and the Indian Ocean during El Niño decaying summer. The other teleconnection is the Silk Road teleconnection, which is forced by Indian monsoon heating and a propagation of stationary Rossby waves along the Asian jet in the upper troposphere over the Asian continent. It can significantly influence the precipitation over north China and the Yangtze River valley and Japan. The Silk Road pattern is a regional manifestation of a circumglobal teleconnection and appears preferentially in summers preceding the peak phases of the cycle when an Indian monsoon precipitation anomaly is evident.
4) NW China is an arid–semiarid area. The surface heating of the TP is the main forcing of local drought. When the surface heating of the TP is weaker than normal, the South Asian high at 100 hPa is located west of 100°E, and an anomalous anticyclone dominant at 500 hPa and westerly jet at 200 hPa in the north of the TP is stronger than normal. They lead to stronger descending motion over NW China and local drought. Although both ENSO and AO show significant correlations with NW China drought, the underlying mechanisms are yet to be elucidated.
5) In terms of the long-term trend and underlying physical mechanisms of East Asian drought from

1950 to the present, a zonal dipole pattern of drought trend is seen over China, with an increasing drought trend over north China and a decreasing tendency over NW China. Drought in northern China is mainly caused by the decreased precipitation and intensified by the increasing temperature and accompanied by decreased EASM and flooding in southern China. The increasing drought in north China in the second half of the twentieth century is consistent with the weakening tendency of EASM, which is driven by the phase transition of the PDO. Anthropogenic agents may only play complementary roles in shaping the monsoon and thereby drought changes in China.

6) Studies on the predictability of East Asian drought are limited, while most prediction studies focus on precipitation and circulation over East Asia. AMIP-type simulations and seasonal hindcasts of climate models show limited skill in simulating the climatological position, annual cycle, and interannual variations of East Asian summer precipitation. In contrast, the circulation related to the interannual variation of East Asian precipitation can be predicted well. ENSO and a good reproduction of the associated teleconnection are the main sources of prediction. Under the SRES A1B scenario and doubled CO_2 simulations, most climate models project an increasing drought frequency and intensity over East Asia, mainly in southeastern Asia. However, the projection patterns and severity are dependent on the climate model and drought index used. Multimodel intercomparisons and an appropriate choice of drought index are necessary in future studies.

Understanding the variation mechanisms of East Asian droughts and their prediction is a challenging task. In terms of the future of this field, there are some important issues–questions that call for further investigation:

1) A reasonable drought index for NW China needs to be developed, because there is no drought index currently able to represent the drought type and severity of the region. The drought index should also consider the detection of drought onset, end point, and the accumulated effect and relationship between drought and the natural ecosystem.
2) How can we better understand the influence of ENSO on short-term atmospheric variability associated with drought? And besides ENSO, are there any other factors that can contribute to the occurrence of drought in East Asia?
3) Despite many studies having noticed the relationship between NW China drought and ENSO–AO, they have done so largely on the basis of statistical analyses; the underlying mechanisms remain unknown.
4) To date, simulation and prediction studies over East Asia have concentrated on precipitation; the simulation and prediction skills of climate models with respect to East Asian drought are yet to be properly examined.

Acknowledgments. This work was jointly supported by the National Natural Science Foundation of China under Grants 41305072, 41330423, and 41023002, and the open Program of NUIST under Grant KLME1306. We thank Dr. Fengfei Song for providing us with some plots in their papers. The authors thank the anonymous reviewers of this paper for their helpful comments.

REFERENCES

Adler, R. F., and Coauthors, 2003: The Version-2 Global Precipitation Climatology Project (GPCP) monthly precipitation analysis (1979–present). *J. Hydrometeor.,* **4,** 1147–1167, doi:10.1175/1525-7541(2003)004<1147:TVGPCP>2.0.CO;2.

An, S., and J. Xing, 1986: A modified Palmer's Drought Index (in Chinese). *J. Acad. Meteor. Sci.,* **1,** 75–82.

Barriopedro, D., C. M. Gouveia, R. M. Trigo, and L. Wang, 2012: The 2009/10 drought in China: Possible causes and impacts on vegetation. *J. Hydrometeor.,* **13,** 1251–1267, doi:10.1175/JHM-D-11-074.1.

Burke, E. J., and S. J. Brown, 2008: Evaluating uncertainties in the projection of future drought. *J. Hydrometeor.,* **9,** 292–299, doi:10.1175/2007JHM929.1.

——, ——, and N. Christidis, 2006: Modeling the recent evolution of global drought and projections for the twenty-first century with the Hadley Centre climate model. *J. Hydrometeor.,* **7,** 1113–1125, doi:10.1175/JHM544.1.

Byun, H. R., and D. A. Wilhite, 1999: Objective quantification of drought severity and duration. *J. Climate,* **12,** 2747–2756, doi:10.1175/1520-0442(1999)012<2747:OQODSA>2.0.CO;2.

Chen, H., T. Zhou, R. B. Neale, X. Wu, and G. J. Zhang, 2010: Performance of the new NCAR CAM3.5 in East Asian summer monsoon simulations: Sensitivity to modifications of the convection scheme. *J. Climate,* **23,** 3657–3675, doi:10.1175/2010JCLI3022.1.

Dai, A., 2011a: Drought under global warming: A review. *Wiley Interdiscip. Rev.: Climate Change,* **2,** 45–65, doi:10.1002/wcc.81.

——, 2011b: Characteristics and trends in various forms of the Palmer drought severity index during 1900–2008. *J. Geophys. Res.,* **116,** D12115, doi:10.1029/2010JD015541.

——, 2013: Increasing drought under global warming in observations and models. *Nat. Climate Change,* **3,** 52–58, doi:10.1038/nclimate1633.

——, K. E. Trenberth, and T. R. Karl, 1998: Global variations in droughts and wet spells: 1900–1995. *Geophys. Res. Lett.,* **25,** 3367–3370, doi:10.1029/98GL52511.

——, ——, and T. T. Qian, 2004: A global dataset of Palmer drought severity index for 1870–2002: Relationship with soil moisture and effects of surface warming. *J. Hydrometeor.,* **5,** 1117–1130, doi:10.1175/JHM-386.1.

Ding, Q., and B. Wang, 2005: Circumglobal teleconnection in the Northern Hemisphere summer. *J. Climate,* **18,** 3483–3503, doi:10.1175/JCLI3473.1.

——, ——, J. M. Wallace, and G. Branstator, 2011: Tropical–extratropical teleconnections in boreal summer: Observed interannual variability. *J. Climate,* **24,** 1878–1896, doi:10.1175/2011JCLI3621.1.

Ding, Y. H., and Y. Sun, 2003: Inter-decadal variation of the temperature and precipitation patterns in East Asian monsoon region. *Proc. Int. Symp. on Climate Change (ISCC),* Beijing, China, World Meteorological Organization, 66–71.

Duan, A., and G. Wu, 2008: Weakening trend in the atmospheric heat source over the Tibetan Plateau during recent decades. Part I: Observations. *J. Climate,* **21,** 3149–3164, doi:10.1175/2007JCLI1912.1.

Dutra, E., L. Magnusson, F. Wetterhall, H. L. Cloke, G. Balsamo, S. Boussetta, and F. Pappenberger, 2013: The 2010–2011 drought in the Horn of Africa in ECMWF reanalysis and seasonal forecast products. *Int. J. Climatol.,* **33,** 1720–1729, doi:10.1002/joc.3545.

Edwards, D. C., and T. B. McKee, 1997: Characteristics of 20th century drought in the United States at multiple time scales. Department of Atmospheric Science, Colorado State University, Atmospheric Science Paper 634, 155 pp.

Enomoto, T., B. J. Hoskins, and Y. Matsuda, 2003: The formation mechanism of the Bonin high in August. *Quart. J. Roy. Meteor. Soc.,* **129,** 157–178, doi:10.1256/qj.01.211.

Fan, G. Z., and G. D. Cheng, 2003a: Reason analysis of the influence of Qinghai–Xizang Plateau uplifting on arid climate forming in northwest China (I): Influence on general circulation of atmosphere (in Chinese). *Plateau Meteor.,* **22,** 45–57.

——, and ——, 2003b: Simulation of influence of Qinghai–Xizang Plateau uplifting on NW China arid climate forming (II): Changing of atmosphere hydrological cycle and dynamical and thermal effects of Plateau (in Chinese). *Plateau Meteor.,* **22,** 58–66.

Ferguson, I. M., J. A. Dracup, P. B. Duffy, P. Pegion, and S. Schubert, 2010: Influence of SST forcing on stochastic characteristics of simulated precipitation and drought. *J. Hydrometeor.,* **11,** 754–769, doi:10.1175/2009JHM1132.1.

Gao, X. J., D. Zhang, Z. Chen, J. S. Pal, and F. Giorgi, 2007: Land use effects on climate in China as simulated by a regional climate model. *Sci. China,* **50D,** 620–628, doi:10.1007/s11430-007-2060-y.

Gill, A. E., 1980: Some simple solutions for heat-induced tropical circulation. *Quart. J. Roy. Meteor. Soc.,* **106,** 447–462, doi:10.1002/qj.49710644905.

Gong, D. Y., 2007: Climate of China. *Climate Disasters,* S. W. Wang and W. Li, Eds., China Meteor. Press, 138–176.

——, and C. H. Ho, 2003: Arctic oscillation signals in the East Asian summer monsoon. *J. Geophys. Res.,* **108,** 4066, doi:10.1029/2002JD002193.

Guo, Q., 1992: Teleconnection between the floods/droughts in North China and Indian summer monsoon rainfall (in Chinese). *Acta Geogr. Sin.,* **47,** 394–402.

He, B., A. F. Lü, J. Wu, L. Zhao, and M. Liu, 2011: Drought hazard assessment and spatial characteristics analysis in China. *J. Geogr. Sci.,* **21,** 235–249, doi:10.1007/s11442-011-0841-x.

Heim, R. R., Jr., 2000: Drought indices: A review. *Drought: A Global Assessment,* D. A. White, Ed., Hazards and Disasters, Vol. 2, Routledge, 159–167.

Hu, Z. Z., 1997: Interdecadal variability of summer climate over East Asia and its association with 500 hPa height and global sea surface temperature. *J. Geophys. Res.,* **102,** 19 403–19 412, doi:10.1029/97JD01052.

Huang, R. H., J. L. Chen, and G. Huang, 2007: Characteristics and variations of the East Asian monsoon system and its impacts on climate disasters in China. *Adv. Atmos. Sci.,* **24,** 993–1023, doi:10.1007/s00376-007-0993-x.

——, ——, L. Wang, and Z. D. Lin, 2012: Characteristics, processes, and causes of the spatio-temporal variabilities of the East Asian monsoon system. *Adv. Atmos. Sci.,* **29,** 910–942, doi:10.1007/s00376-012-2015-x.

Kalnay, E., and Coauthors, 1996: The NCEP/NCAR 40-Year Reanalysis Project. *Bull. Amer. Meteor. Soc.,* **77,** 437–470, doi:10.1175/1520-0477(1996)077<0437:TNYRP>2.0.CO;2.

Kang, I. S., J. Y. Lee, and C. K. Park, 2004: Potential predictability of summer mean precipitation in a dynamical seasonal prediction system with systematic error correction. *J. Climate,* **17,** 834–844, doi:10.1175/1520-0442(2004)017<0834:PPOSMP>2.0.CO;2.

Keyantash, J., and J. A. Dracup, 2002: The quantification of drought: An evaluation of drought indices. *Bull. Amer. Meteor. Soc.,* **83,** 1167–1180, doi:10.1175/1520-0477(2002)083<1191:TQODAE>2.3.CO;2.

Kim, D. W., and H. R. Byun, 2009: Future pattern of Asian drought under global warming scenario. *Theor. Appl. Climatol.,* **98,** 137–150, doi:10.1007/s00704-008-0100-y.

——, ——, and K. S. Choi, 2009: Evaluation, modification, and application of the effective drought index to 200-year drought climatology of Seoul, Korea. *J. Hydrol.,* **378,** 1–12, doi:10.1016/j.jhydrol.2009.08.021.

——, ——, ——, and S. B. Oh, 2011: A spatiotemporal analysis of historical droughts in Korea. *J. Appl. Meteor. Climatol.,* **50,** 1895–1912, doi:10.1175/2011JAMC2664.1.

Kim, H. M., P. J. Webster, J. A. Curry, and V. E. Toma, 2012: Asian summer monsoon prediction in ECMWF System 4 and NCEP CFSv2 retrospective seasonal forecasts. *Climate Dyn.,* **39,** 2975–2991, doi:10.1007/s00382-012-1470-5.

Kosaka, Y., and H. Nakamura, 2006: Structure and dynamics of the summertime Pacific–Japan teleconnection pattern. *Quart. J. Roy. Meteor. Soc.,* **132,** 2009–2030, doi:10.1256/qj.05.204.

——, J. S. Chowdary, S. P. Xie, Y. M. Min, and J. Y. Lee, 2012: Limitations of seasonal predictability for summer climate over East Asia and the northwestern Pacific. *J. Climate,* **25,** 7574–7589, doi:10.1175/JCLI-D-12-00009.1.

Lee, J., S. Lee, B. Wang, K. Ha, and J. Jhun, 2013: Seasonal prediction and predictability of the Asian winter temperature variability. *Climate Dyn.,* **41,** 573–587, doi:10.1007/s00382-012-1588-5.

Lee, S.-M., H.-R. Byun, and H. L. Tanaka, 2012: Spatiotemporal characteristics of drought occurrences over Japan. *J. Appl. Meteor. Climatol.,* **51,** 1087–1098, doi:10.1175/JAMC-D-11-0157.1.

Li, B., and T. J. Zhou, 2011: El Niño–Southern Oscillation–related principal interannual variability modes of early and late summer rainfall over East Asia in sea surface temperature-driven atmospheric general circulation model simulations. *J. Geophys. Res.,* **116,** D14118, doi:10.1029/2011JD015691.

Li, H., A. Dai, T. Zhou, and J. Lu, 2010: Responses of East Asian summer monsoon to historical SST and atmospheric forcing during 1950–2000. *Climate Dyn.,* **34,** 501–514, doi:10.1007/s00382-008-0482-7.

Li, S., R. Liu, L. Shi, and Z. Ma, 2009: Analysis on drought characteristic of He'nan in recent 40 years based on meteorological drought composite index. *J. Arid Meteor.,* **27,** 97–102.

Li, S. L., J. Lu, G. Huang, and K. M. Hu, 2008: Tropical Indian Ocean basin warming and East Asian summer monsoon: A multiple AGCM study. *J. Climate,* **21,** 6080–6088, doi:10.1175/2008JCLI2433.1.

Li, Y. H., and D. L. Li, 2004: Effects of ENSO cycle on the summer climate anomaly over northwest China (in Chinese). *Plateau Meteor.,* **23,** 930–935.

Lin, R., T. Zhou, and Y. Qian, 2014: Evaluation of global monsoon precipitation changes based on five reanalysis datasets. *J. Climate,* **27,** 1271–1289, doi:10.1175/JCLI-D-13-00215.1.

Liu, H., T. Zhou, Y. Zhu, and Y. Lin, 2012: The strengthening East Asia summer monsoon since the early 1990s. *Chin. Sci. Bull.,* **57,** 1553–1558, doi:10.1007/s11434-012-4991-8.

Liu, W., S. An, G. Liu, and A. Guo, 2004: The further modification of the Palmer Drought Severity Model (in Chinese). *J. Appl. Meteor. Sci.,* **15,** 207–216.

Liu, X., S. Yang, Q. Li, A. Kumar, S. Weaver, and S. Liu, 2014: Subseasonal forecast skills and biases of global summer monsoons in the NCEP Climate Forecast System version 2. *Climate Dyn.,* **42,** 1487–1508, doi:10.1007/s00382-013-1831-8.

Liu, X. M., J. Li, Z. H. Lu, M. Liu, and W. R. Xing, 2009: Dynamic changes of composite drought index in Liaoning Province in recent 50 years (in Chinese). *Chin. J. Ecol.,* **28,** 938–942.

Liu, Y., and Y. Ding, 2008: Analysis and numerical simulations of the teleconnection between Indian summer monsoon and precipitation in North China (in Chinese). *Acta Meteor. Sin.,* **22,** 489–501.

Luo, L., and E. F. Wood, 2007: Monitoring and predicting the 2007 U.S. drought. *Geophys. Res. Lett.,* **34,** L22702, doi:10.1029/2007GL031673.

——, W. Tang, Z. Lin, and E. Wood, 2013: Evaluation of summer temperature and precipitation predictions from NCEP CFSv2 retrospective forecast over China. *Climate Dyn.,* **41,** 2213–2230, doi:10.1007/s00382-013-1927-1.

Ma, Z., 2007: The interdecadal trend and shift of dry/wet over the central part of North China and their relationship to the Pacific Decadal Oscillation (PDO). *Chin. Sci. Bull.,* **52,** 2130–2139, doi:10.1007/s11434-007-0284-z.

——, and C. Fu, 2006: Some evidence of drying trend over northern China from 1951 to 2004. *Chin. Sci. Bull.,* **51,** 2913–2925, doi:10.1007/s11434-006-2159-0.

Man, W., T. Zhou, and J. H. Jungclaus, 2012: Simulation of the East Asian summer monsoon during the last millennium with the MPI Earth System Model. *J. Climate,* **25,** 7852–7866, doi:10.1175/JCLI-D-11-00462.1.

Mao, R., D. Gong, and Q. Fang, 2007: Influences of the East Asian jet stream on winter climate in China (in Chinese). *J. Appl. Meteor. Sci.,* **18,** 137–146.

Matsuno, T., 1966: Quasi-geostrophic motions in the equatorial area. *J. Meteor. Soc. Japan,* **44,** 25–43.

McKee, T. B., N. J. Doesken, and J. Kleist, 1993: The relationship of drought frequency and duration to time scales. *Proc. 8th Conf. on Applied Climatology,* Anaheim, CA, Amer. Meteor. Soc., 179–184.

Menon, S., J. Hansen, L. Nazarenko, and Y. Luo, 2002: Climate effects of black carbon aerosols in China and India. *Science,* **27,** 2250–2253, doi:10.1126/science.1075159.

Mishra, A. K., and V. P. Singh, 2010: A review of drought concepts. *J. Hydrol.,* **391,** 202–216, doi:10.1016/j.jhydrol.2010.07.012.

Mitchell, T. D., and P. D. Jones, 2005: An improved method of constructing a database of monthly climate observations and associated high resolution grids. *Int. J. Climatol.,* **25,** 693–712, doi:10.1002/joc.1181.

Morid, S., V. Smakhtin, and M. Moghaddasi, 2006: Comparison of seven meteorological indices for drought monitoring in Iran. *Int. J. Climatol.,* **26,** 971–985, doi:10.1002/joc.1264.

Nitta, T., 1987: Convective activities in the tropical western Pacific and their impact on the Northern Hemisphere summer circulation. *J. Meteor. Soc. Japan,* **65,** 373–390.

North, G., T. L. Bell, R. F. Cahalan, and F. J. Moeng, 1982: Sampling errors in the estimation of empirical orthogonal functions. *Mon. Wea. Rev.,* **110,** 699–706, doi:10.1175/1520-0493(1982)110<0699:SEITEO>2.0.CO;2.

Oh, S.-B., H.-R. Byun, and D.-W. Kim, 2014: Spatiotemporal characteristics of regional drought occurrence in East Asia. *Theor. Appl. Climatol.,* **117,** 89–101, doi:10.1007/s00704-013-0980-3.

Palmer, W. C., 1965: Meteorologic drought. U.S. Department of Commerce, Weather Bureau, Research Paper 45, 58 pp.

Pandey, R. P., B. B. Dash, S. K. Mishra, and R. Singh, 2007: Study of indices for drought characterization in KBK districts in Orissa (India). *Hydrol. Processes,* **22,** 1895–1907, doi:10.1002/hyp.6774.

Qian, C., and T. Zhou, 2014: Multidecadal variability of North China aridity and its relationship to PDO during 1900–2010. *J. Climate,* **27,** 1210–1222, doi:10.1175/JCLI-D-13-00235.1.

Qian, W., and Y. L. Zhu, 2001: Climate change in China from 1880 to 1998 and its impact on the environmental condition. *Climatic Change,* **50,** 419–444, doi:10.1023/A:1010673212131.

——, Q. Hu, Y. Zhu, and D.-K. Lee, 2003: Centennial-scale dry–wet variations in East Asia. *Climate Dyn.,* **21,** 77–89, doi:10.1007/s00382-003-0319-3.

Qiu, H. J., M. Cao, J. Hao, Y. Wang, and Y. Wang, 2013: Relationship between frequency and magnitude of drought damage in China in 1950–2010. *Sci. Geogr. Sin.,* **33,** 576–580.

Qiu, J., 2010: China drought highlights future climate threats. *Nature,* **465,** 142–143, doi:10.1038/465142a.

Sato, N., and M. Takahashi, 2006: Dynamical processes related to the appearance of quasi-stationary waves on the subtropical jet in the midsummer Northern Hemisphere. *J. Climate,* **19,** 1531–1544, doi:10.1175/JCLI3697.1.

Sheffield, J., and E. Wood, 2008: Projected changes in drought occurrence under future global warming from multi-model, multi-scenario, IPCC AR4 simulations. *Climate Dyn.,* **31,** 79–105, doi:10.1007/s00382-007-0340-z.

Shen, C. M., W. C. Wang, Z. Hao, and W. Dong, 2007: Exceptional drought events over eastern China during the last five centuries. *Climatic Change,* **85,** 453–471, doi:10.1007/s10584-007-9283-y.

Shi, Y., Y. Shen, E. Kang, D. Li, Y. Ding, G. Zhang, and R. Hu, 2007: Recent and future climate change in northwest China. *Climatic Change,* **80,** 379–393, doi:10.1007/s10584-006-9121-7.

Sillman, J., V. V. Kharin, F. W. Zwiers, X. Zhang, and D. Bronaugh, 2013: Climate extremes indices in the CMIP5 multimodel ensemble: Part 2. Future climate projections. *J. Geophys. Res. Atmos.,* **118,** 2473–2493, doi:10.1002/jgrd.50188.

Song, F., and T. Zhou, 2013: FGOALS-s2 simulation of upper-level jet streams over East Asia: Mean state bias and synoptic-scale transient eddy activity. *Adv. Atmos. Sci.,* **30,** 739–753, doi:10.1007/s00376-012-2212-7.

——, and ——, 2014: Interannual variability of East Asian summer monsoon simulated by CMIP3 and CMIP5 AGCMs: Skill dependence on Indian Ocean–western Pacific anticyclone teleconnection. *J. Climate,* **27,** 1679–1697, doi:10.1175/JCLI-D-13-00248.1.

——, ——, and Y. Qian, 2014: Responses of East Asian summer monsoon to natural and anthropogenic forcings in the 17 latest CMIP5 models. *Geophys. Res. Lett.,* **41,** 596–603, doi:10.1002/2013GL058705.

Sperber, K. R., H. Annamalai, I.-S. Kang, A. Kitoh, A. Moise, A. Turner, B. Wang, and T. Zhou, 2013: The Asian summer monsoon: An intercomparison of CMIP5 vs. CMIP3 simulations of the late 20th century. *Climate Dyn.,* **41,** 2711–2744, doi:10.1007/s00382-012-1607-6.

Sun, C., and S. Yang, 2012: Persistent severe drought in southern China during winter–spring 2011: Large-scale circulation patterns and possible impacting factors. *J. Geophys. Res.,* **117,** D10112, doi:10.1029/2012JD017500.

Takaya, K., and H. Nakamura, 2001: A formulation of a phase-independent wave-activity flux for stationary and migratory quasigeostrophic eddies on a zonally varying basic flow. *J. Atmos. Sci.,* **58,** 608–627, doi:10.1175/1520-0469(2001)058<0608:AFOAPI>2.0.CO;2.

Vicente-Serrano, S. M., S. Beguería, and J. I. López-Moreno, 2010: A multiscalar drought index sensitive to global warming: The standardized precipitation evapotranspiration index. *J. Climate,* **23,** 1696–1718, doi:10.1175/2009JCLI2909.1.

Wang, A., D. P. Lettenmaier, and J. Sheffield, 2011: Soil moisture drought in China, 1950–2006. *J. Climate,* **24,** 3257–3271, doi:10.1175/2011JCLI3733.1.

Wang, B., and Z. Fan, 1999: Choice of South Asian summer monsoon indices. *Bull. Amer. Meteor. Soc.,* **80,** 629–638, doi:10.1175/1520-0477(1999)080<0629:COSASM>2.0.CO;2.

——, and Q. Ding, 2006: Changes in global monsoon precipitation over the past 56 years. *Geophys. Res. Lett.,* **33,** L06711, doi:10.1029/2005GL025347.

——, R. Wu, and T. Li, 2003: Atmosphere–warm ocean interaction and its impacts on Asian–Australian monsoon variation. *J. Climate,* **16,** 1195–1211, doi:10.1175/1520-0442(2003)16<1195:AOIAII>2.0.CO;2.

——, Q. Ding, X. Fu, I.-S. Kang, K. Jin, J. Shukla, and F. Doblas-Reyes, 2005: Fundamental challenge in simulation and prediction of summer monsoon rainfall. *Geophys. Res. Lett.,* **32,** L15711, doi:10.1029/2005GL022734.

——, J. Yang, T. Zhou, and B. Wang, 2008: Interdecadal changes in the major modes of Asian–Australian monsoon variability: Strengthening relationship with ENSO since the late 1970s. *J. Climate,* **21,** 1771–1789, doi:10.1175/2007JCLI1981.1.

——, and Coauthors, 2009: Advance and prospectus of seasonal prediction: Assessment of the APCC/CliPAS 14-model ensemble retrospective seasonal prediction (1980–2004). *Climate Dyn.,* **33,** 93–117, doi:10.1007/s00382-008-0460-0.

Wang, H., 2001: The weakening of Asian monsoon circulation after the end of 1970's. *Adv. Atmos. Sci.,* **18,** 376–386, doi:10.1007/BF02919316.

Wang, J., J. Guo, Y. Zhou, and L. Yang, 2007: Progress and prospect on drought indices research (in Chinese). *Arid Land Geogr.,* **30,** 60–65.

Wang, P. X., J. H. He, Y. F. Zheng, and Q. Zhang, 2007: Interdecadal relationship between summer Arctic Oscillation and aridity–wetness feature in northwest China (in Chinese). *J. Desert Res.,* **27,** 883–889.

Wang, S. W., D. Gong, J. Ye, and Z. Chen, 2000: Seasonal precipitation series over China since 1880 (in Chinese). *Acta Geogr. Sin.,* **55,** 281–293.

——, J. Cai, and J. Zhu, 2002: The interdecadal variations of annual precipitation in China during 1880s–1990s (in Chinese). *Acta Meteor. Sin.,* **60,** 637–639.

Wang, T., H. Wang, O. Ottera, Y. Gao, L. Suo, T. Furevik, and L. Yu, 2013: Anthropogenic agent implicated as a prime driver of shift in precipitation in eastern China in the late 1970s. *Atmos. Chem. Phys.,* **13,** 12 433–12 450, doi:10.5194/acp-13-12433-2013.

Wang, W., H. Xu, 2012: The modification of Palmer drought severity index in the research of drought in the Huaihe area. *Adv. Earth Sci.,* **27,** 60–67, doi:10.11867/j.issn.1001-8166.2012.01.0060.

Wang, Z., and Y. Ding, 2006: Climate change of the cold wave frequency of China in the last 53 years and the possible reasons (in Chinese). *Chin. J. Atmos. Sci.,* **30,** 1068–1076.

Wei, K., and L. Wang, 2013: Reexamination of the aridity conditions in arid northwestern China for the last decade. *J. Climate,* **26,** 9594–9602, doi:10.1175/JCLI-D-12-00605.1.

Wu, B., T. Zhou, and T. Li, 2009: Seasonally evolving dominant interannual variability modes of East Asian climate. *J. Climate,* **22,** 2992–3005, doi:10.1175/2008JCLI2710.1.

——, T. Li, and T. Zhou, 2010: Relative contributions of the Indian Ocean and local SST anomalies to the maintenance of the western North Pacific anomalous anticyclone during the El Niño decaying summer. *J. Climate,* **23,** 2974–2986, doi:10.1175/2010JCLI3300.1.

Wu, R., and B. P. Kirtman, 2005: Roles of Indian and Pacific Ocean air–sea coupling in tropical atmospheric variability. *Climate Dyn.,* **25,** 155–170, doi:10.1007/s00382-005-0003-x.

——, and ——, 2007: Regimes of seasonal air–sea interaction and implications for performance of forced simulations. *Climate Dyn.,* **29,** 393–410, doi:10.1007/s00382-007-0246-9.

——, Z. Hu, and B. Kirtman, 2003: Evolution of ENSO-related rainfall anomalies in East Asia. *J. Climate,* **16,** 3742–3758, doi:10.1175/1520-0442(2003)016<3742:EOERAI>2.0.CO;2.

Wu, T., and Z. Qian, 1996: Comparative analyses of differences between circulation and dynamical effect of Qinghai–Xizang Plateau over NW China drought area in dry- and wet-summer. *Plateau Meteor.,* **15,** 387–396.

——, ——, P. Li, M. Song, and X. Ma, 1998: Some comparative analyses of subsequent precipitation over northwest China drought area in winter heavy- and light-snow years over Qinghai–Xizang Plateau (in Chinese). *Plateau Meteor.,* **17,** 364–372.

Xiao, J., Q. Zhuang, E. Liang, X. Shao, A. D. McGuire, A. Moody, D. W. Kicklighter, and J. M. Melillo, 2009: Twentieth-century drought and their impacts on terrestrial carbon cycling in China. *Earth Interact.,* **13,** doi:10.1175/2009EI275.1.

Xie, S.-P., K. Hu, J. Hafner, H. Tokinaga, Y. Du, G. Huang, and T. Sampe, 2009: Indian Ocean capacitor effect on Indo–western Pacific climate during the summer following El Niño. *J. Climate,* **22,** 730–747, doi:10.1175/2008JCLI2544.1.

Xin, X. G., R. Yu, T. Zhou, and B. Wang, 2006: Drought in late spring of South China in recent decades. *J. Climate,* **19,** 3197–3206, doi:10.1175/JCLI3794.1.

——, T. Zhou, and R. Yu, 2010: Increased Tibetan Plateau snow depth: An indicator of the connection between enhanced winter NAO and late-spring tropospheric cooling over East Asia. *Adv. Atmos. Sci.,* **27,** 788–794, doi:10.1007/s00376-009-9071-x.

Xu, G. C., and Z. Y. Zhang, 1983: The effect of Qinghai–Xizang Plateau on the formation of dry climate over the northwest China (in Chinese). *Plateau Meteor.,* **2,** 9–16.

Xu, K., D. Young, H. Yang, Z. Li, Y. Qin, and Y. Shen, 2014: Spatio-temporal variation of drought in China during 1961–2012: A climatic perspective. *J. Hydrol.,* doi:10.1016/j.jhydrol.2014.09.047, in press.

Xu, Q., 2001: Abrupt change of the mid-summer climate in central east China by the influence of atmospheric pollution. *Atmos. Environ.,* **35,** 5029–5040, doi:10.1016/S1352-2310(01)00315-6.

Yang, J., D. Gong, W. Wang, M. Hu, and R. Mao, 2012: Extreme drought event of 2009/2010 over southwestern China. *Meteor. Atmos. Phys.,* **115,** 173–184, doi:10.1007/s00703-011-0172-6.

Yang, L. F., and W. S. Xie, 2009: Drought-flood monitoring and index test in Anhui Province (in Chinese). *J. Anhui Agric. Sci.,* **37,** 3848–3850.

Yang, S., Z. Zhang, V. Kousky, R. Higgins, S. Yoo, J. Liang, and Y. Fan, 2008: Simulations and seasonal prediction of the Asian summer monsoon in the NCEP Climate Forecast System. *J. Climate,* **21,** 3755–3775, doi:10.1175/2008JCLI1961.1.

Yang, X., G. Liu, X. Yang, and R. Wang, 2005a: The modification of Palmer Drought Severity Model for Gansu Loess Plateau (in Chinese). *Arid Meteor.,* **23,** 8–12.

——, X. Yang, P. Ma, R. Wang, and Y. Dong, 2005b: Modification and applications of PDSI for mid and eastern Gansu Province (in Chinese). *Adv. Earth Sci.,* **20,** 1022–1028.

Yao, Y., C. Zhang, Z. Deng, A. Dong, X. Zhang, F. Wei, and J. Yang, 2007: Overview of meteorological and agricultural drought indices (in Chinese). *Agric. Res. Arid Areas,* **25,** 185–189.

Ye, D. Z., and Y. X. Gao, 1979: *Tibetan Plateau Meteorology* (in Chinese). Science Press, 278 pp.

Yu, R. C., and T. J. Zhou, 2007: Seasonality and three-dimensional structure of the interdecadal change in East Asian monsoon. *J. Climate,* **20,** 5344–5355, doi:10.1175/2007JCLI1559.1.

——, B. Wang, and T. Zhou, 2004: Tropospheric cooling and summer monsoon weakening trend over East Asia. *Geophys. Res. Lett.,* **31,** L22212, doi:10.1029/2004GL021270.

Yuan, W. P., and G. S. Zhou, 2004: Theoretical study and research prospect on drought indices (in Chinese). *Adv. Earth Sci.,* **19,** 982–991.

Yuan, X., and E. F. Wood, 2013: Multimodel seasonal forecasting of global drought onset. *Geophys. Res. Lett.,* **40,** 4900–4905, doi:10.1002/grl.50949.

Zhai, J., B. Su, V. Krysanova, T. Vetter, C. Gao, and T. Jiang, 2010: Spatial variation and trends in PDSI and SPI indices and their relation to streamflow in 10 large regions of China. *J. Climate,* **23,** 649–663, doi:10.1175/2009JCLI2968.1.

Zhang, C., B. Wang, D. Liu, and Z. Cai, 1998: Research on drought and flood indices in the northwest China (in Chinese). *Plateau Meteor.,* **17,** 381–389.

Zhang, L. X., and T. Zhou, 2011: An assessment of monsoon precipitation changes during 1901–2001. *Climate Dyn.,* **37,** 279–296, doi:10.1007/s00382-011-0993-5.

Zhang, Q., J. Wei, and S. Tao, 2003: The decadal and interannual variations of drought in the northern China and association with the circulations (in Chinese). *Climate Environ. Res.,* **8,** 318–328.

——, X. Zou, and F. Xiao, 2006: Classification of meteorological droughts. Standards Press of China Tech. Rep. GB/T20481-2006, 17 pp.

——, and Coauthors, 2009: *Drought* (in Chinese). China Meteorological Press, 199 pp.

Zhang Q., J. F. Li, V. P. Singh, and Y. G. Bai, 2012: SPI-based evaluation of drought events in Xinjiang, China. *Nat. Hazards,* **64,** 481–492, doi:10.1007/s11069-012-0251-0.

Zhang, S. Y., and Coauthors, 2008: *Arid Meteorology* (in Chinese). China Meteorological Press, 292 pp.

Zhou, T. J., and R. C. Yu, 2005: Atmospheric water vapor transport associated with typical anomalous summer rainfall patterns in China. *J. Geophys. Res.,* **110,** D08104, doi:10.1029/2004JD005413.

——, and L. Zou, 2010: Understanding the predictability of East Asian summer monsoon from the reproduction of land–sea thermal contrast change in AMIP-type simulation. *J. Climate,* **23,** 6009–6026, doi:10.1175/2010JCLI3546.1.

——, and T. Hong, 2013: Projected changes of Palmer drought severity index under an RCP8.5 scenario. *Atmos. Oceanic Sci. Lett.,* **6,** 273–278, doi:10.3878/j.issn.1674-2834.13.0032.

——, R. Yu, H. Li, and B. Wang, 2008a: Ocean forcing to changes in global monsoon precipitation over the recent half-century. *J. Climate,* **21,** 3833–3852, doi:10.1175/2008JCLI2067.1.

——, L. Zhang, and H. Li, 2008b: Changes in global land monsoon area and total rainfall accumulation over the last half century. *Geophys. Res. Lett.,* **35,** L16707, doi:10.1029/2008GL034881.

——, D. Gong, J. Li, and B. Li, 2009a: Detecting and understanding the multi-decadal variability of the East Asian summer monsoon—Recent progress and state of affairs. *Meteor. Z.,* **18,** 455–467, doi:10.1127/0941-2948/2009/0396.

——, B. Wu, and B. Wang, 2009b: How well do atmospheric general circulation models capture the leading modes of the interannual variability of the Asian–Australian monsoon? *J. Climate,* **22,** 1159–1173, doi:10.1175/2008JCLI2245.1.

——, F. Song, R. Lin, X. Chen, and X. Chen, 2013: The 2012 North China floods: Explaining an extreme rainfall event in the context of a long-term drying tendency [in ''Explaining Extreme Events of 2012 from a Climate Perspective'']. *Bull. Amer. Meteor. Soc.,* **94** (9), S49–S51.

Zhu, Y. L., H. J. Wang, W. Zhou, and J. Ma, 2011: Recent changes in the summer precipitation pattern in East China and the background circulation. *Climate Dyn.,* **36,** 1463–1473, doi:10.1007/s00382-010-0852-9.

Zou, X., and Q. Zhang, 2008: Preliminary studies on variations in droughts over China during past 50 years (in Chinese). *J. Appl. Meteor. Sci.,* **19,** 679–687.

——, P. Zhai, and Q. Zhang, 2005: Variations in droughts over China: 1951–2003. *Geophys. Res. Lett.,* **32,** L04707, doi:10.1029/2004GL021853.